ABSTRACT

Biometrics is the development of statistical and mathematical methods applicable to data analysis problems in the biological sciences. It is a new method of verifying authenticity. Biometrics uses biological traits or behavioral characteristics to identify an individual. A Biometrics system is actually a pattern recognition system that utilizes various patterns like iris patterns, retina patterns and biological traits like fingerprints, facial geometry, voice recognition and hand recognition etc. What makes Biometrics really attractive is the fact that the various security codes like the passwords and the PIN can be interchanged between people but the physiological traits can't be.

The current applications of Biometric authentication are Entry control, ATM's and Government programs. The most obvious use of biometrics for network security is for secure workstation logons for a workstation connected to a network. The main use of Biometric network security will be to replace the current password system. The most popular biometric authentication scheme employed for the last few years has been Iris Recognition. Many companies are adding biometric authentication features to their products for e.g. Key ware Technologies LBV (Layered biometrics verification) Internet toolkit provides high-level security to e-commerce applications. This toolkit finds use in the area of Internet Banking.

ACKNOWLEDGEMENT

We would like to take this opportunity to thank everyone whose cooperation and encouragement throughout the ongoing course of this project remains invaluable to us.

We are sincerely grateful to our guide and mentor **Prof.Nilanjana Dutta Roy** of the Department of **Computer Science & Engineering, IEM Kolkata**, for her wisdom, guidance and inspiration that helped us go through with this project and take it to where it stands now.

We would also like to express our sincere gratitude to **Prof.Satyajit Chakraborty, Director,Prof. Dr. Amlan Kusum Nayak, Principal and Prof. Dr. Debika Bhattacharyya**, HOD of Computer Science & Engineering and other faculties of Institute of Engineering & Management, for their assistance and encouragement.

Last but not the least, we would like to extend our warm regards to our families and peers who have kept supporting us and always had faith in our work.

Sushmita Goswami

Reg. No :121040110118 of 2012-2013

&

Suchismita Goswami

Reg. No :121040110241 of 2012-2013

TABLE OF CONTENTS

LIST OF FIGURES

LIST OF TABLES

CHAPTER 1. INTRODUCTION

1.1 OBJECTIVE

The objective of this project is to make an autonomous biometric security system which can be used to prevent attacks in various sensitive areas like airport,banks,passport system etc. Traditional authentication systems which use identification id, a password and many more is highly prone to risk . Emerging technologies demand for more reliable and comfortable user authentication methods . Automated biometric systems for personal authentication is among these newly adopted techniques .Biometric reorganization technology relies upon the physical characteristics of individual such as fingerprint , palm print etc. All of these technologies suffer from interference because of dirtiness ,roughness or injury of the organs to be used for authentication purpose .Hence these are not stable and accurate . Retinal biometrics , being considered as one of the most reliable biometrics among all, are majorly used when the issue of very high security arises. Mostly, the biometric parameter employed for the retinal authentication is its vessel configuration , acquired through retinal digital fundus images of human eye, because of its uniqueness for each individual. With the rapid growth of retinal biometrics for authentication, searching an efficient feature is essentially important and challenging task for faster and safer execution .Thus using the unique biometric features of the retinal images we will generate a template which will be used as the main authentication key for this autonomous security .Existing systems are time consuming process, takes minimum 15 seconds time to adjust camera with human eye. It's not accepted. Moreover, one cannot move their head. Images captured from different angles may lead to even authentication failure . In the proposed system this problem can be resolved as the relative features of different biometric parameters of retinal image have been considered.

1.2 SCOPE:

The problem that this system is going to solve is described as follows-

- **Airport** :- Today's passenger and cabin baggage security screening works, but at great cost to authorities, to the airline industry, and to passengers. Given the predicted growth in air travel, continuously evolving security threats, and passengers being increasingly dissatisfied with queues and intrusive measures . Moreover carry-on-items of the passengers are checked through dual-energy X-ray system, but the checking of the identity of travellers is done by checking a photo ID, such as a driver's license ,passport etc .Simply taking a look at a photo ID isn't enough .In the proposed system travellers do not need to carry any smart card with him/her and the entire system would work without intervention of any security guard .This system can seeks to deliver strengthened security , Increased operational efficiency ,Improved passenger experience etc.
- **Banks**:- In banking system usually the account number or pin number and the signature is used for enabling security measures .The fraudster then uses this information to carry out fraudulent transactions in countries where chip and PIN technology is not supported .The fraudster may also use this information in transactions where the card doesn't have to be physically seen by the retailer or merchant. For example, when shopping online .Proposed system provides another security layer in addition to the existing measures to prevent this spoofing and skimming attacks .The use of biometrics in banking can be used because of its potential as a predominant method of identifying themselves to access banking services such as branch banking, online banking, ATM networks, and mobile banking.

- **Passport**:- The duplicate passport problem can also be resolved through this proposed system.

- **Terrorist Attack**:- Now-a-days it is very much common that prisoners sometimes fled away from prison .If some facial changes takes place due to plastic surgery it become very difficult to identify though that person is suspiciously caught again for his behaviour.
- Proposed system can be used to provide biometric security to the homeowners.
- **Medical Analysis**:- This System can be used for earlier detection of PDR(Proliferative Diabetic Retinopathy).

1.3 ORGANIZATION

CHAPTER 1: INTRODUCTION: Gives a brief introduction on what is being done and why this topic has been chosen.

CHAPTER 2: BACKGROUND: In this section we shall discuss a literature survey of projects done on similar topics and how the authors tried to achieve their objective.

CHAPTER 3: SEGMENTATION OF BLOOD VESSELS: In this section, the method of segmenting the blood vessels has been described.

CHAPTER 4: LOCALIZATION OF OPTIC DISC: In this section , the method of localizing the center of optic disc has been described.

CHAPTER 5: LOCALIZATION OF MACULA: In this section, the method of localizing the center of macula has been described.

CHAPTER 6: COMPUTATION OF WIDTH OF THE BLOOD VESSEL: In this section, method to calculate the width of blood vessels, the ratio of parent vessels and child vessels, detection of PDR has been described.

CHAPTER 7: EXTRACTION OF DISTINCT BIFURCATION POINTS: In this section, method to identify the distinct bifurcation has been described.

CHAPTER 8: GENERATION OF TEMPLATE: In this section, the method to generate the 96 bytes template from all extracted features from the retinal images has been described.

CHAPTER 9: CONCLUSION: The limitation of our framework and future scope of the work i.e. where and how we can improve this technique to make it more suitable.

CHAPTER 2 .BACKGROUND

2.1 BASIC CONCEPT OF BIOMETRIC TEMPLATE GENERATION

Biometric system is essentially a pattern recognition system which recognizes a user by determining the authenticity of a specific physiological or behavioral characteristic possessed by the user. Several important issues must be considered in designing a practical biometric system. First, a user must be enrolled in the system so that his biometric template can be captured. This template is securely stored in a central database or a smart card issued to the user. The template is retrieved when an individual needs to be identified. Depending on the context, a biometric system can operate either in a verification (authentication) or an identification mode.

Verification Vs Identification:

There are two different ways to resolve a person's identity: verification and identification. Verification (Am I whom I claim I am?) involves confirming are denying a person's claimed identity. In identification, one has to establish a person's identity (Who am I?). Each one of these approaches has its own complexities and could probably be solved best by a certain biometric system.

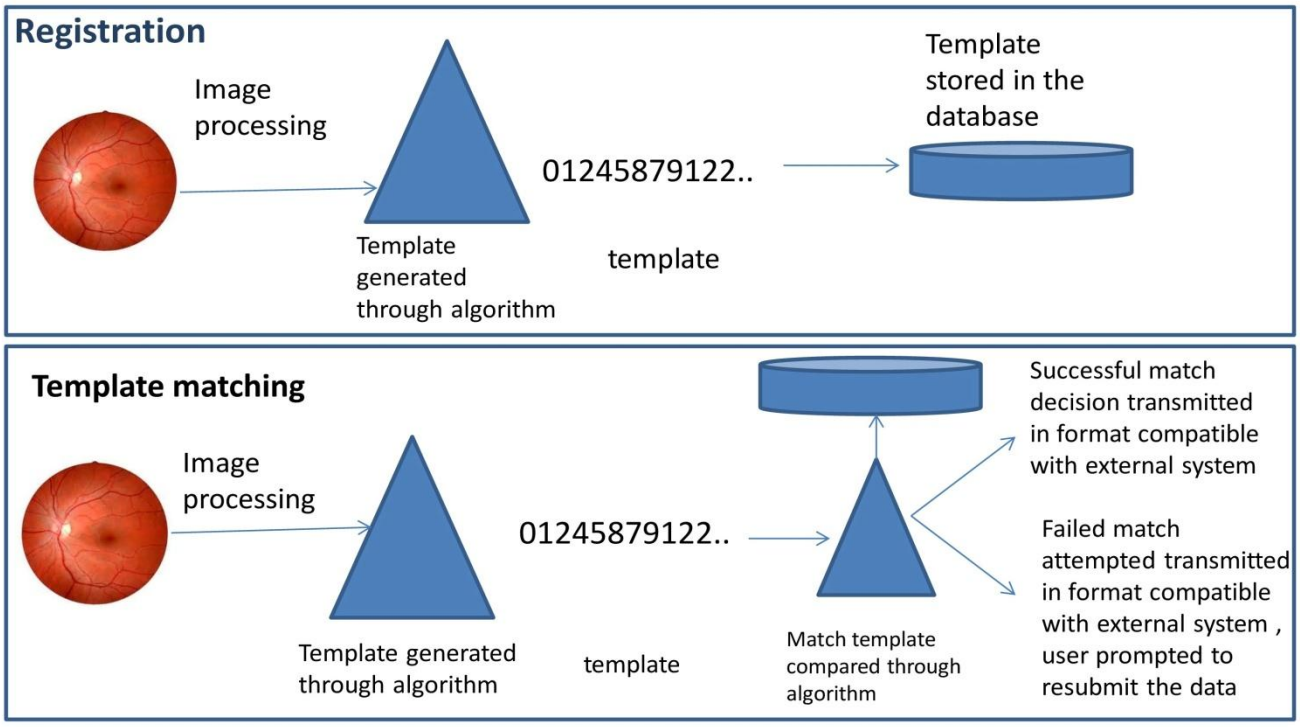

Figure 1: image showing the block diagram of the system

2.2 RELATED LITERATURE REVIEW:

Alauddin Bhuiyan ,Tien Wong et al. in their paper named A NEW AND EFFICIENT METHOD FOR AUTOMATIC OPTIC DISCDETECTION USING GEOMETRICAL FEATURES , they presented a method for OD detection which is based on image global intensity levels, OD size and shape analysis. According to them ,firstly the OD is the brightest part on the image and hence they had approximated its pixel intensity values by analyzing the histogram. Secondly ,OD is more or less circular shaped and they have specified its size within a particular range for any person .

Sourav Saha , Nilanjana Dutta Roy et al. [2] have proposed a novel method for automatic detection of bifurcation points in retinal fundus-images .They have focused on determining the potential bifurcation points by analyzing local neighborhood connectivity around junction points on blood-vessels.

Tracking-based approaches utilize a profile model to incrementally step along and segment a vessel. Vessel tracking a one-dimensional matched filter fell with a given threshold. The tracking method was driven by a fuzzy model of a one-dimensional vessel profile [3]. One drawback to these approaches is their dependence upon methods for locating the starting points, which must always be either at the optic nerve or at subsequently detected branch points.

Many image processing methods proposed for retinal vessels extraction [4] [5] [6] [7] [8] . Optimized Gabor filters with local entropy thresholding had been used in those approaches for segmentation of the blood vessels in the retinal images. The drawback of those segmentation methodology is that Optimized Gabor filter methods often produce false positive detections and fail to detect vessel of different widths. Also detection process much more complicated when retinal image abnormal condition.

An automated texture based blood vessels segmentation has been proposed in the paper[14] .In this paper they have used Fuzzy c-Means(FCM) clustering algorithm for the classification between vessels and non - vessels depending on texture properties. This algorithm is having 84.37% sensitivity and 99.19% specificity .

G. Kavitha MIT , S. Ramakrishnan et. al. in their paper named " Identification and analysis of macula in retinal images using Ant Colony Optimization based hybrid method" has presented a method of localization of macula in which the fundus retinal images are subjected to ant colony optimization (ACO) based method to identify optic disc (OD) and Otsu method to further analyze the macula. Parameters such as radius of optic disc and distance between the centers of the optic disc and macula are used as indices for evaluation.

A novel method has been proposed by the authors of [5] for detection of vascular bifurcations along with crossovers from color retinal fundus images. In this method, the retinal images are converted to segmented images using color-space transformation, Fuzzy C-Means and texture analysis. Then the potential crossover and bifurcation points are scanned by using a rotational invariant mask on the centreline image. The main problem with this approach is that during segmentation some blood vessels are failed to get segmented which results in the loss of possible bifurcation points. Moreover, separation of bifurcation and crossover points cannot be implemented by this algorithm.

A method for detection of crossover points has also been proposed in [6]. Ini- tially, they have considered the retinal image as their input and from the vascular network of it, a skeleton image has been extracted. Next, in the analysis phase of each pixel, they have scanned the skeleton image to check for a bifurcation and crossover point. Presence of two close bifurcations has been considered as a single crossover point. Finally, geometrical features are analyzed to detect the false crossover points. However, the disadvantage is that for any vessel less than 5 pixels of width, this method may fail to identify that particular crossover point.

The authors of [7] have proposed an approach to perform image registration. The bifurcation points are identified by scanning the $3*3$ neighbors of each pixel and identifying a T-like shape. The disadvantage is that if the distance

between the two arms of a bifurcation point is less than 5 pixel it is removed and if points that are very close they are detected as trifurcation.

Li has [8] proposed an approach to detect vascular bifurcations and crossovers in fundus images. In this approach, the Gaussian filter in implemented to re- duce the central reflex to the blue channel of the original retinal image. The knowledge of structure and direction is obtained by eigen values and eigenvectors of Hessian Matrix. A multi scale vessel filter is defined that uses the response of bifurcations and crossovers, by using the isotropic and anisotropic values of the pixels. The isotropy as well as the anisotropy of the neighboring segments is computed for each pixel and used for defining a multi-scale vessel filter.

George et al. [12] developed a method for automatic detection of vascular bifurcations in segmented retinal images. Trainable filters are implemented in this method that behave similar to the Shape-selective neurons in V4 of visual cortex.

In another literature [9], the authors have proposed a method for automatic ex- traction of blood vessels, bifurcation as well as end points in the vascular tree in retinal images. Initially, an anisotropic diffusion filter is introduced followed by a matched filter to enhance blood vessels. A kernel appropriate for the filter is also developed that can rotate in all possible directions.

Lowell et al. [13] proposed a deformable contour model to segment the optic nerve head boundary in low resolution retinal images. The approach localizes the optic disc using a specialised template matching and a directionally-sensitive gradient to eliminate the obstruction of the vessel in the optic disc region before performing the segmentation.

Welfer et al. [14] proposed an automated segmentation of the optic disc in colour eye fundus image using an adaptive morphological operation. The method uses a watershed transform markers to define the optic disc boundary and the vessel obstruction is minimized by morphological erosion.

CHAPTER 3: SEGMENTATION OF BLOOD VESSELS

3.1 BLOCK DIAGRAM

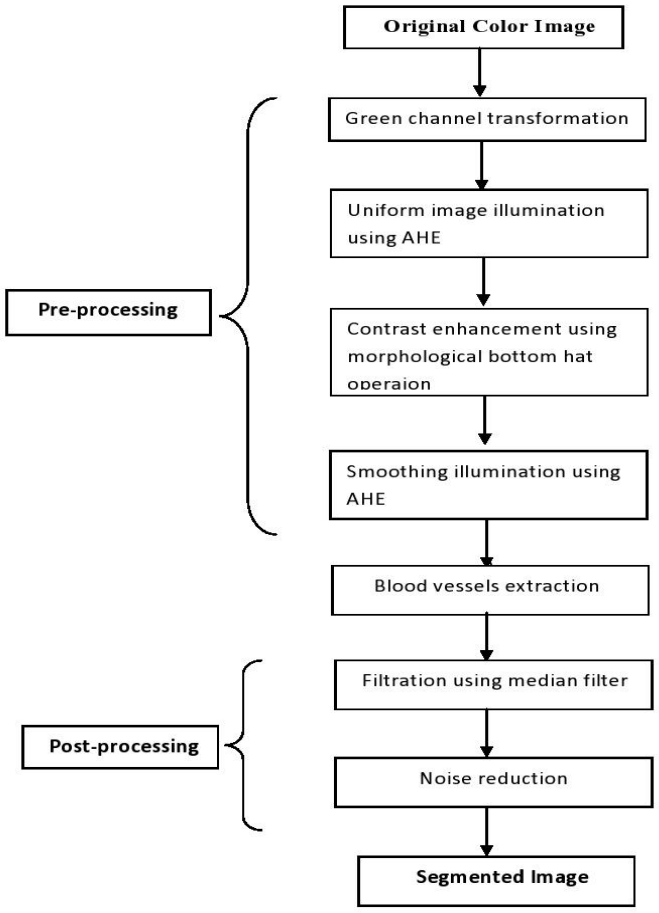

3.2 ALGORITHM

Algorithm 1: Segmentation of blood vessels from retinal fundus image

Input: RBG Retinal Image.
Output: Segmented Image of blood vessel.

Step1: RGB image is converted into Green channel.
Step2: Boundary of the previously obtained green channel image is being removed.
Step 3: Contrast of the image is enhanced by contrast-limited adaptive histogram equalization.
Step 4: Then morphological "bottom hat" operation is performed with structuring element of size 8X8.
Step 5: The image obtained after preprocessing is converted to binary image using threshold value obtained by Otsu's method of thresholding.
Step 6: Median filter is used to remove salt & paper noise from previously obtained image.
Step 7: Next, smaller object is removed and final segmented blood vessel is obtained.

3.3 EXPLANATION

3.3.1 Preprocessing:

The retinal images have non uniform illumination of the background due to the presence of vitreous humor, which is a transparent gel that fills the interior of the eye. The blood vessels have varying thickness and contrast due to which the darker vessels (thick vessels) can be easily detected which it is difficult to extract the vessels having poor contrast (thin vessels).So it is desirable to have high contrast between the retinal blood vessels and retinal background whilst there should be low contrast between retinal background and retinal abnormalities so that the blood vessel tree appears as dark structure in brighter background in the images. Hence preprocessing is applied to the original retinal image in order to eliminate these anomalies to prepare the image for the next steps of segmentation algorithm for detection the blood vessels to higher accuracy.

The preprocessing stage of the proposed algorithm is splitted into 5 steps. Steps are described as follows -

3.3.1.1 Channel Conversion:- The input image is a color (RGB) image. The red channel is the brightest color channel and has low contrast. The green channel provides the best vessel background contrast of the RGB representation. So the green channel of the image is extracted from the original RGB retinal images. Please refer Figure 2:

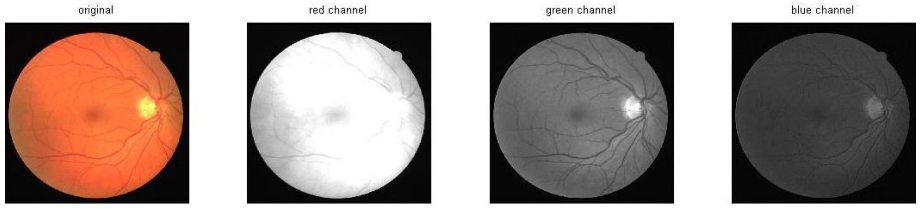

(a) (b) (c) (d)

Figure 2*(a):original RGB image,(b)red channel image,(c)green channel image,(d)blue channel image(left to right)*

3.3.1.2 Boundary Removal: - In this step the outer border of the green component of the image is removed by suppressing the structures that are lighter that the surroundings and that are connected to the image border.

3.3.1.3 Blood Vessel Enhancement: - Fundus images have background intensity variation due to non uniform illumination which may deteriorate the segmentation result. Due this non uniformity in the image Background pixels may have their gray levels higher than the vessel pixels. So in this phase global thresholding techniques cannot be applied due to the various gray levels in different areas in the image and noisy unconnected regions appeared as false vessels Hence Contrast-limited adaptive histogram equalization is applied for enhancing the contrast of the green channel retinal image to redistribute the lightness value of the image .This enhancement operation is performed on the small regions of the image , instead of the entire image and thus contrast of every smaller region is enhanced .Please refer Figure 3(a) ,Figure 3(b) ,Figure 4(a) and Figure 4(b),

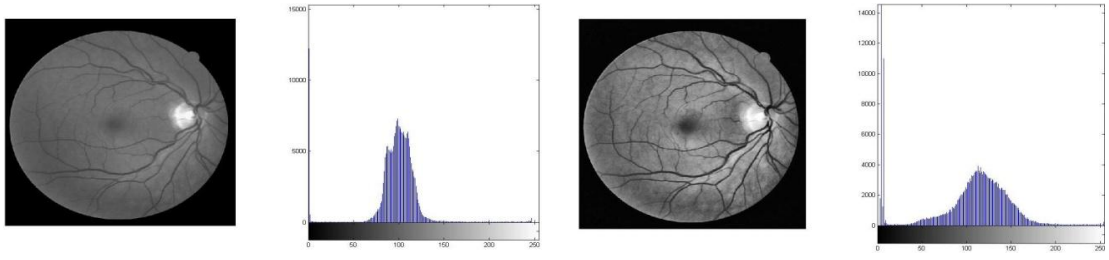

(a) (b) (a) (b)

Figure 3*(a): green channel image, (b) its Histogram*

Figure 4*(a) AHE filtered image (b) its histogram,*

This step helps to reduce some responses from abnormalities which do not resemble any blood vessels that would otherwise decrease the performance of blood vessels segmentation method.

3.3.1.4 <u>Morphological Transformation</u>:- As in some cases blood vessels appeared as part of the background in a binary image due to the less intensity difference between blood vessels and image background , morphological bottom hat operation is performed in order to improve the contrast with a disk shaped structuring element of size 8x8.the shape and the size of the structuring element is set according to the image structure that are to be extracted. Bottom-hat filtering subtracts the input image from the result of performing a morphological closing operation on the image. Closing operation is defined s dilation (Max filter) followed by erosion (Min filter).Please refer Figure 5.

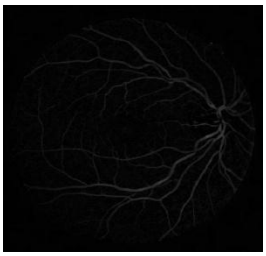

Figure *5:showing image after morphological bottom hat operation*

3.3.1.5 <u>Smoothing Illumination</u>:-The image produced after the bottom hat operation has poor contrast. Hence In order to improve the contrast again contrast-limited adaptive histogram equalization is applied so that the image is well prepared for thresholding and segmentation stage. Please refer Figure 6, Figure 7.

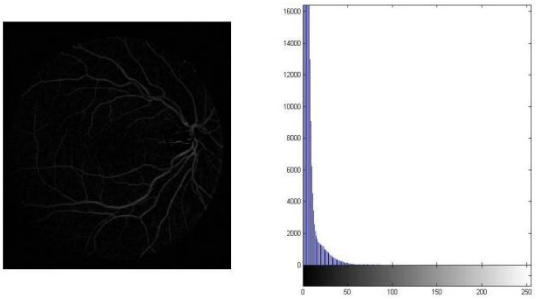

Figure 6*: image after bottom hat& its histogram*

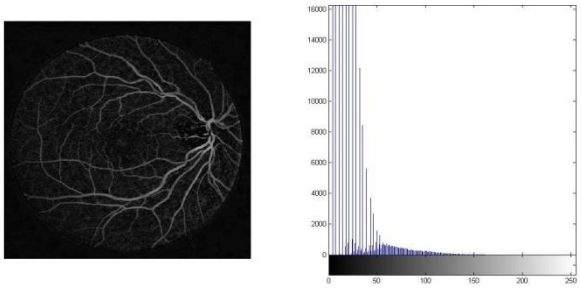

Figure 7*:contrast enhanced image & its histogram*

3.3.2 <u>Blood Vessels Segmentation:-</u> Preprocessing step has enhanced the contrast of the original image. Hence after enhancing the signal of the blood vessels which is lying in the range below the threshold value, the image is thresholded using the OTSU algorithm keeping the information below the threshold value and giving the rest of the image the same value as the threshold. Thus cluster based algorithm is used to perform clustering based image thresholding and the preprocessed gray scale image is reduced into the binary image. Please refer Figure 8.

Otsu's method is used to automatically perform clustering based image <u>thresholding</u> to reduce the gray level image into the binary image. In Otsu's method threshold value is used which minimizes the intra-class variation, defined as a weighted sum of variances of the two classes.

$$\sigma^2_w(t) = \omega_0(t)\,\sigma^2_0(t) + \omega_1(t)\,\sigma^2_1(t) \quad (1)$$

Weights $\omega_{0,1}$ are the probabilities of the two classes separated by a threshold t and $\sigma^2_{0,1}$ are variances of these two classes[11].

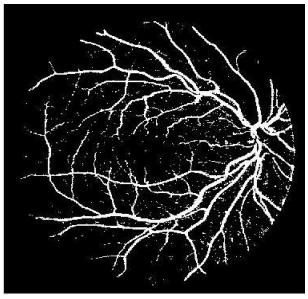

Figure8: *showing extracted blood vessels after applying Otsu's method of thresholding*

3.3.3.**<u>Post Processing</u>**:-

3.3.3.1 <u>Noise Removal</u>: - The image obtained by previous stages contains salt & paper noise. Hence a 2-D median filter with 3-by-3 neighborhood size is applied to obtain a clear image with a minimum extent of the noise of the green channel .Each output pixel contains the median value in a 3-by-3 neighborhood around the corresponding pixel in the input image .Please refer Figure 9(a).

Next, all the small connected components that have fewer than 35 white pixels around it within the 8x8 connectivity are removed from the previously processed image to get the final segmented image .Please refer Figure 9(b).

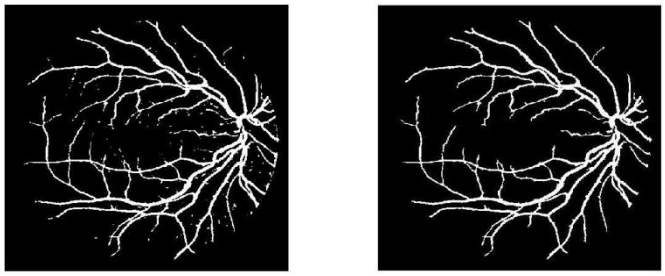

(a) (b)

Figure9 *(a) Median filtered image ,(b) segmented image after noise removal*

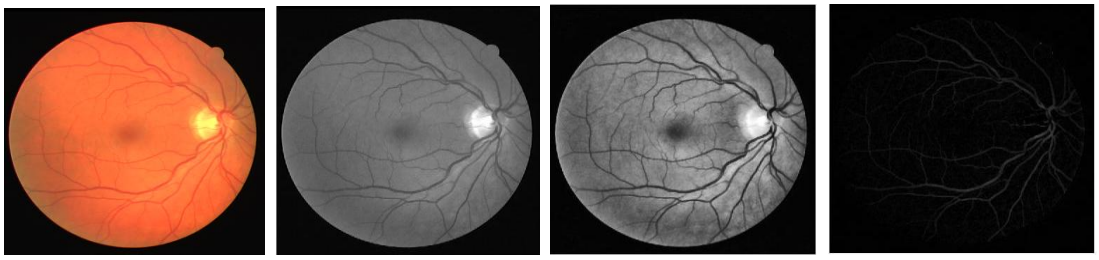

(a) (b) (c) (d)

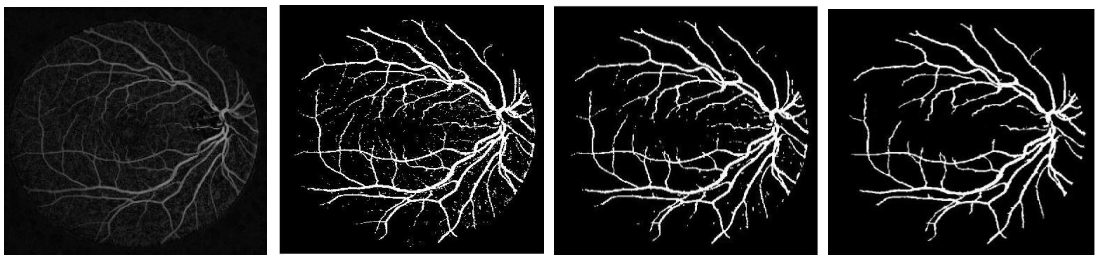

***Figure 10**: (a) Original RGB image ,(b) green channel image ,(c) AHE filtered image ,(d) after performing bottom hat operation ,(e) contrast enhanced image ,(f) extracted blood vessels by Otsu's thresholding ,(g) median filtered image ,(h)segmented image after removing noise*

3.4. EXPERIMENTAL RESULT AND ANALYSIS

3.4.1 EXPERIMENTAL SETUP

To evaluate the performance of the proposed system experiments have been conducted base on the DRIVE[2] and VARIA[3] database. The photographs for the DRIVE database were obtained from a diabetic retinopathy screening program in The Netherlands. Each image was captured using 8 bits per color plane at 768 by 584 pixels. For the training images, a single manual segmentation of the vasculature is available. For the test cases, two manual segmentations are available; one is used as gold standard, the other one can be used to compare computer generated segmentations with those of an independent human observer. The VARIA database is a set of retinal images used for authentication purposes. The database currently includes 233 images, from 139 different individuals. The images are optic disc centered with a resolution of 768x584[3].

3.4.1.1 VARIA SEGMENTATION:

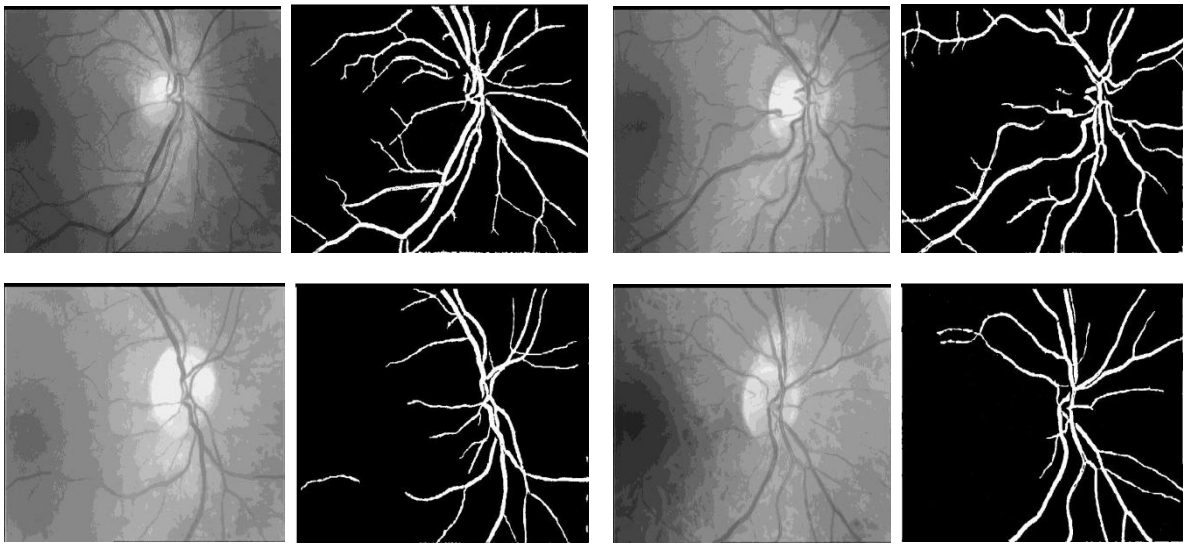

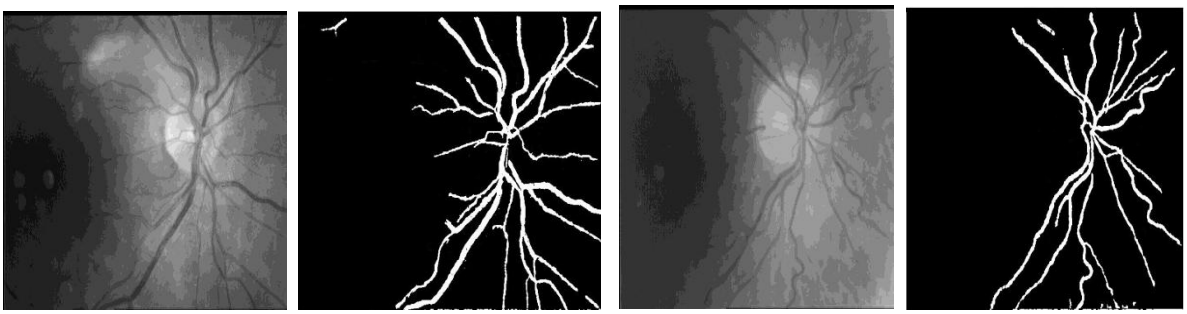

***Figure** 11: original gray scale image & its segmented image(image pair left to right)*

3.4.1.2 DRIVE SEGMENTATION :

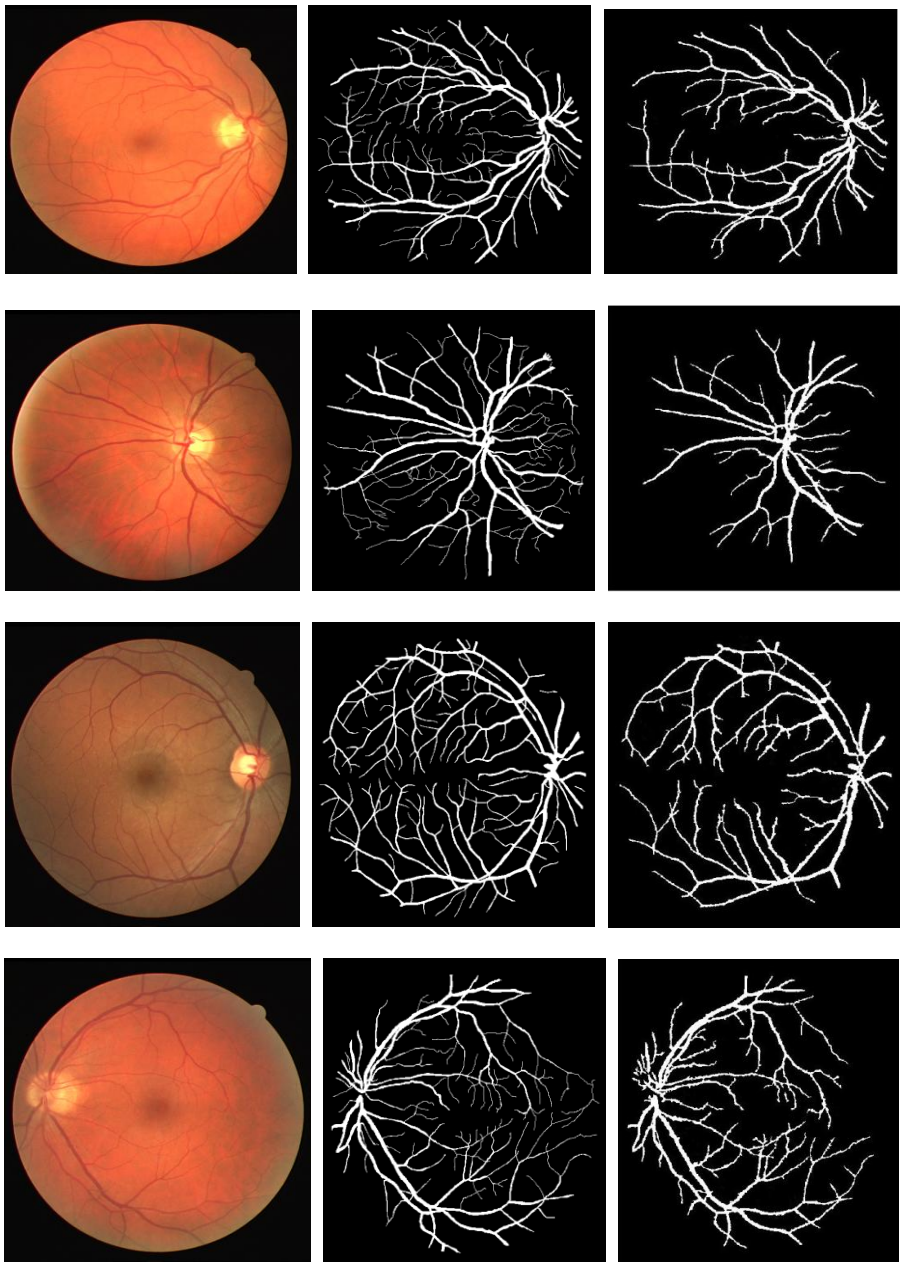

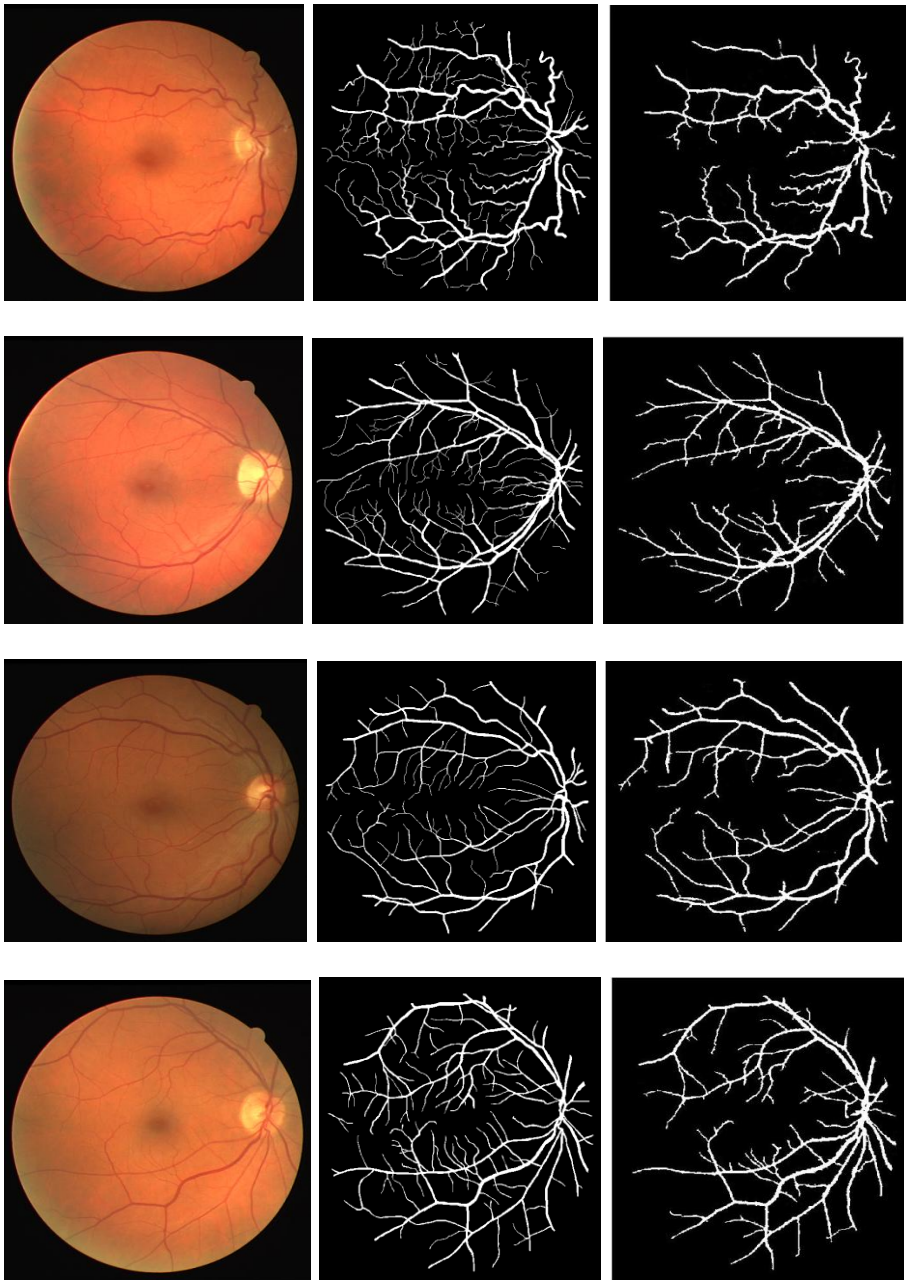

Figure 12 *(a) Original RGB image , (b) hand labeled Gold standard image(ground truth) (c) segmented image by the proposed method(dendrites removed)*

3.4.2 PERFORMANCE EVALUATION METRIC

3.4.2.1 <u>Evaluation Parameter:</u> To evaluate the proposed algorithm manually following parameters are defined in order to compare the results from the algorithm with other algorithms.

- **<u>TP (true positive):</u>** This refers to the pixels of the blood vessels that are correctly recognized by the algorithm. Let TP denotes the number of true positives.

- **FP (false positive)**: This refers to the pixels of the blood vessels that are incorrectly recognized as positive pixels by the algorithm. Let FP denotes the number of false positive.

- **TN (true negative)**: This refers to the pixels of the blood vessels that are correctly discarded by the algorithm. Let TN denotes the number of true negative.

- **FN (false negative)**: This refers to the positive pixels of the blood vessels that were mislabeled as negative pixels by the proposed algorithm. Let FN denotes the number of false negative.

TPR, FPR, TNR and FNR are the other parameters which are also used in evaluation process are defined as follows.

- **TPR (true positive rate):** It is the ratio of the true positives to all pixels belonging to blood vessels. This is also called **SENSITIVITY.**

  Sensitivity = (Number of true positive)/ (Number of true positives + Number of false negative)
  = TP/P
  = (TP)/ (TP+FN) (4)

- **TNR (true negative rate):** It is the ratio of the false positives to all the pixels that do not belong to the blood vessels. This is also known as **SPECIFICITY**.

  Specificity = (Number of true negatives)/ **(**Number of true negatives **+** Number of false positives)
  = TN/N
  = (TN)/ (TN+FP) (5)

- **FPR (false positive rate):** It is the ratio of false positive to all the pixels that do not belong to the blood vessels. This is also known as fall-out.

  Fall-out = (Number of false positive)/ **(**Number of true negatives **+** Number of false positives)
  = FP/N
  = FP/ (TN+FP) (6)

- **FNR (false negative rate): It is t**he ratio of false negative to all the pixels belonging to the blood vessels.

  FNR = (Number of false negative)/ (Number of true positives + Number of false negative)
  = FN/P
  = FN/ (TP+FN) (7)

  Using the above parameters, accuracy of the proposed algorithm has been calculated.

- **Accuracy:** it is a description of systematic errors, a measure of statistical bias. Accuracy of the algorithm is defined as

  Accuracy (ACC) = (∑True Positive + ∑True Negative)/Total population
  = (TP + TN)/ (TP + FN + TN + FP) (8)

3.4.2.2 PROPOSED METHOD (APPLIED ON DRIVE DATABASE)(TABLE 1)

Image sequence	Sensitivity	Accuracy (%)
1	0.944	97.44
2	0.985	98.50
4	1	97.23

12	0.944	96.44
16	1	96.11
19	0.933	96.33
22	0.9167	98.61
27	1	96.90
36	0.928	97.47
40	1	98.33
Average	**0.95897**	**97.33**

3.4.2.3 COMPARISION WITH OTHER SEGMENTATION ALGORITHMS(TABLE 2)

Methodology	Sensitivity(TPR)	Accuracy (%)
Human Observer	0.7763	94.70%
Mendonca et al. [4]	0.7344	94.63%
Niemeije et al. [5]	0.7145	94.16%
Osareh et. al[18]	0.9650	96.75%
Fraz et al[17]	0.7406	94.80%
Marin et al[16]	0.7067	94.52%
Lupascu et al[19]	0.72	95.97%
Xu and Luo[20]	0.7760	93.28%
Ricci and Perfetti [21]	----	95.63%
Proposed method	0.9589	97.33%

3.5 CONCLUSION:

In this paper we have presented a novel approach for automatic blood vessels segmentation technique from retinal fundus image. Proposed algorithm has been tested on publicly available databases like DRIVE[9] and VARIA[10]. we have executed the proposed algorithm on 32 bit Matlab R2013a version on 32 bit Windows 7 running on Intel Core2 dual processor with 2 GB RAM.We have used various contrast enhancement techniques and the morphological operators which aims to provide better segmentation results including both minor and major vessels. This Segmentation algorithm works efficiently with less space and time consumption. We hope that this algorithm can help speed up diagnosis and improve the diagnostic performance of specialized physicians and in security purposes too.

CHAPTER 4: LOCALIZATION OF OPTIC DISC CENTRE:

4.1 BLOCK DIAGRAM

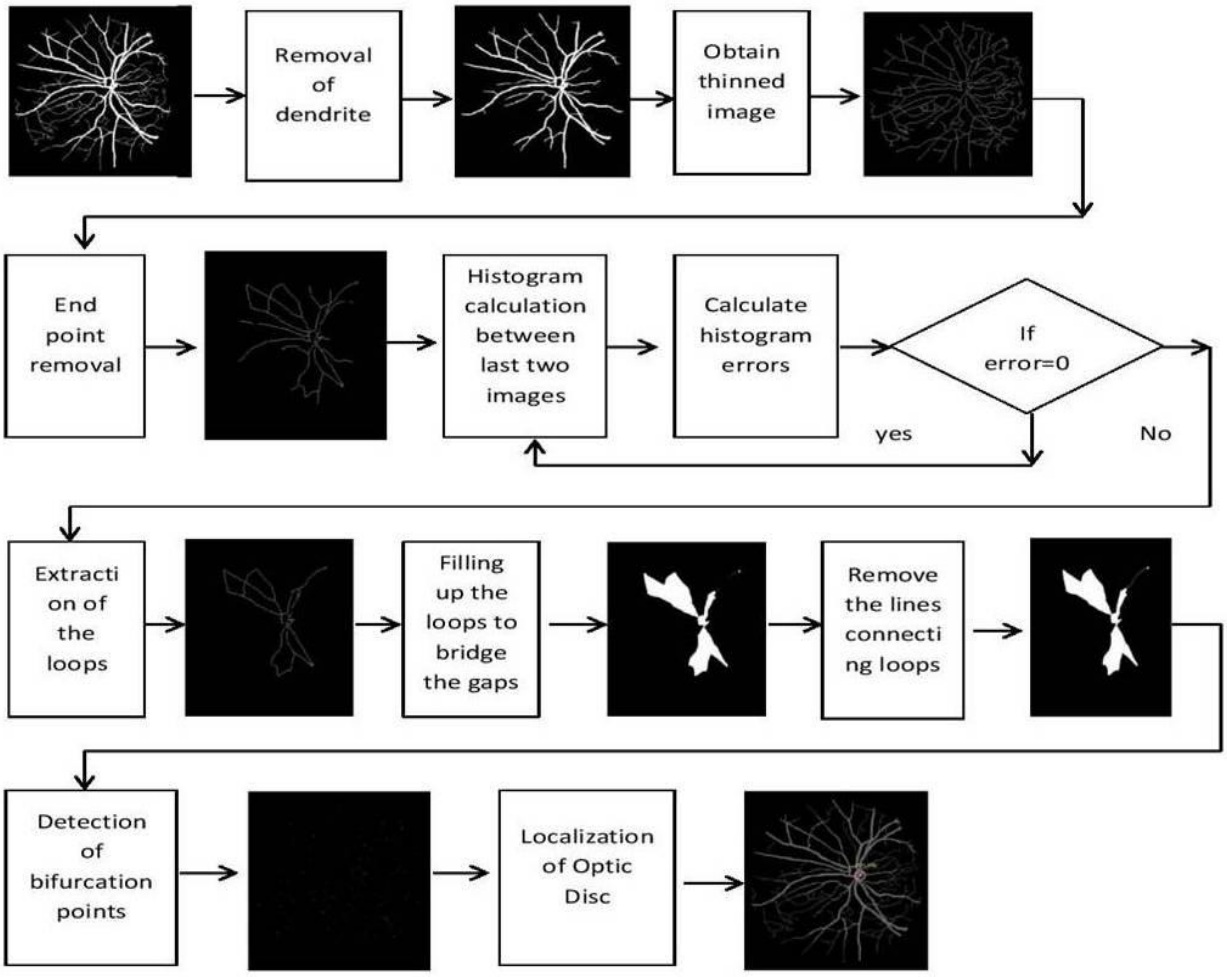

4.2 EXPLAINATION

Proposed Algorithm of Localization of optic disc:-

It has been statistically found from the thinned images, that the overlapping of major blood vessels near optic disc area again forms polygonal loop like structures. We are emphasizing on this loop structure by considering them as the key feature to locate the optic disc in this algorithm. But overlapping of the dendrites may also generate loops which carries redundant information. So removing dendrites is an essential task to keep the loops near the optic disc intact.

Input: - Segmented binary image

Output: - Center of the Optic Disc

Step 1.Removing the dendrites from the segmented image.

Step 2.The morphological thinning operation is performed on the segmented fundus image to get a thinned image .

Step 3. [End points removed] Within an iterative loop, all the end points are removed from the thinned image by checking its all eight neighborhood pixels to be of white colored. Every time the new image is being compared with the previous one obtained from the early iteration by calculating the difference of the histogram of the two images.

If this difference is then two images are exactly equal and no further removal of endpoint is required.

Step 4. After the loop structure is found the thinned lines connecting the loop structures are removed and then the loops are filled up by using matlab defined 'imfill' operation.

Step 5.Now the distance between the all the bifurcation points from the loop structure are calculated .Then the bifurcation points having minimum distance from the loop structure among all, are found as the bifurcations nearer to the optic disc.

Step 6. For each of the previously obtained bifurcation at the end of Step 5, no of bifurcation points around it is calculated. And the bifurcation point which is having the maximum no of bifurcation points around it is considered as the root pixel.

Step 7.Then the no of blood vessels around the optic disc is calculated.

4.3 COMPLEXITY ANALYSIS (OPTIC DISC LOCALIZATION):-

While Finding the center of the optic disc , we have first of all found out the branch point which is done in O(n) time , then the removal of terminal until the loop is found is also done in O(n) time .The distance between a single bifurcation point to the loop is found in O(n) times .So if there is n no of bifurcation points then for all these points, the algorithm would work with time complexity of O(n^2).Next we have considered only those bifurcation points nearer to the optic disc which drastically reduces the complexity of the algorithm . And finally calculation of no of branch points around each of this bifurcation point will be done in O(n) times.

So time complexity for this algorithm is O(n^2). Apart from this there would be obvious need of O(n2) amount of time while scanning the entire image for processing.

As there is no additional space or storage requirement so constant space complexity.

DETECTED CENTER POINT OF THE OPTIC DISC OF THE DRIVE IMAGE :-

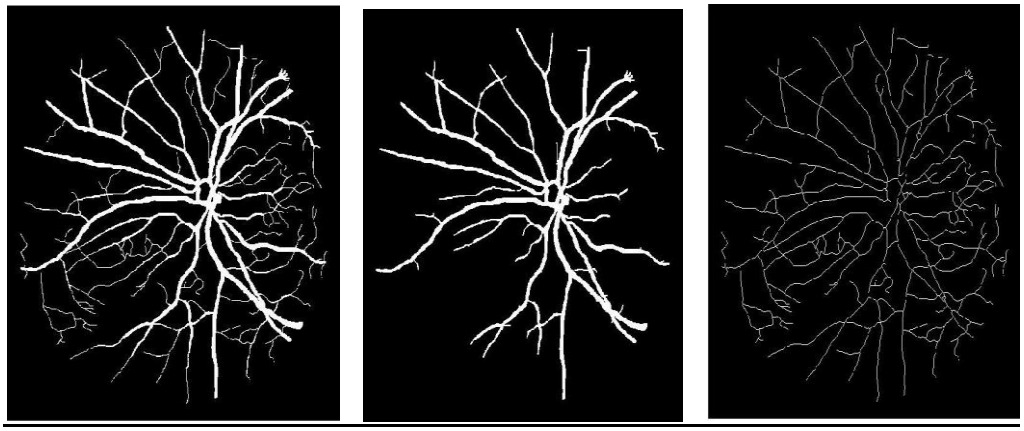

(a) **(b)** **(c)**

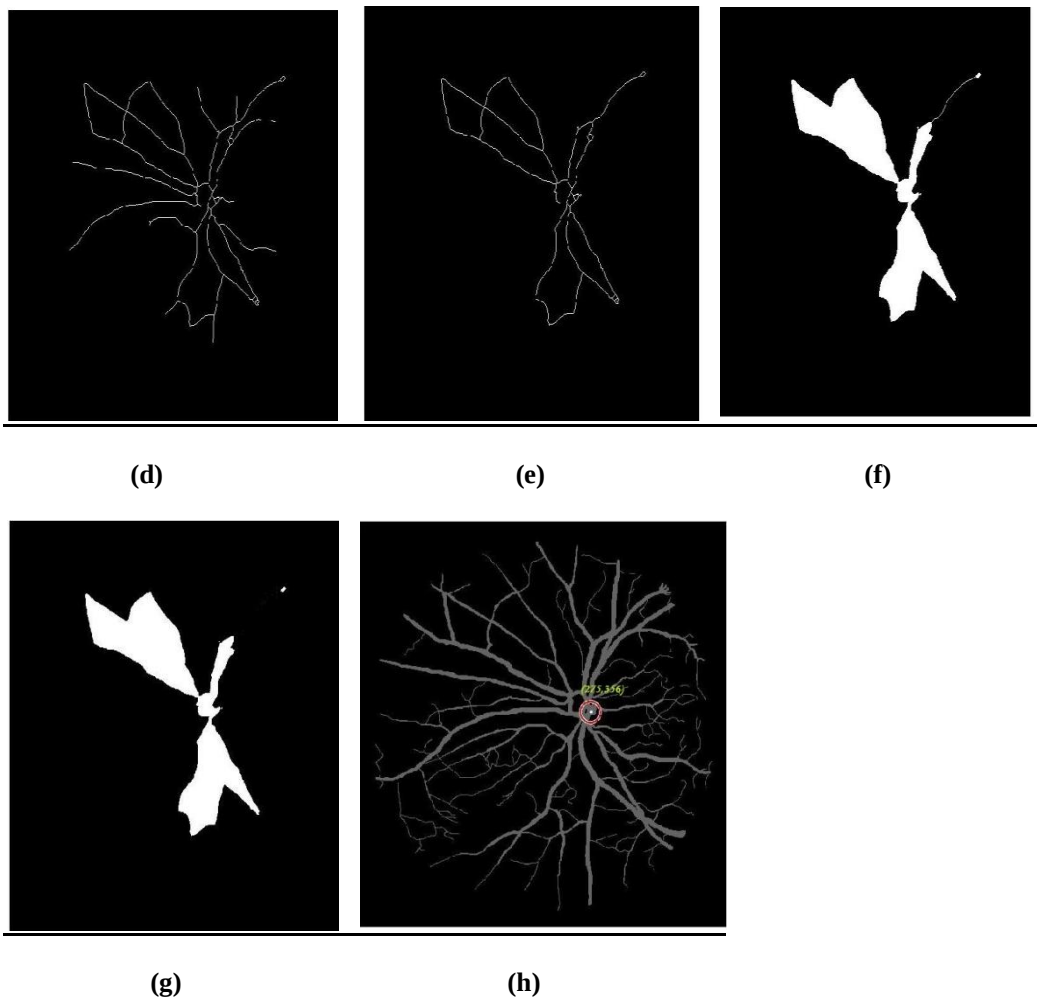

Figure. 13*. (a) segmented fundus image (b) image after removing the dendrites (c) Thinned image obtained after applying morphological function (d)Image after a few iteration (e) after extracting the loops in the image (f) after applying imfill function to bridge the holes (g) after removing lines connecting the loops (h) optic disc located*

4.4. EXPERIMENTAL RESULT AND ANALYSIS

4.4.1 EXPERIMENTAL SETUP

To evaluate the performance of the proposed system experiments have been conducted base on the DRIVE[2] and VARIA[3] database. The photographs for the DRIVE database were obtained from a diabetic retinopathy screening program in The Netherlands. Each image was captured using 8 bits per color plane at 768 by 584 pixels. For the training images, a single manual segmentation of the vasculature is available. For the test cases, two manual segmentations are available; one is used as gold standard, the other one can be used to compare computer generated segmentations with those of an independent human observer. The VARIA database is a set of retinal images used for authentication purposes. The database currently includes 233 images, from 139 different individuals. The images are optic disc centered with a resolution of 768x584[3].

4.4.2 RESULTS ON FUNDUS IMAGES

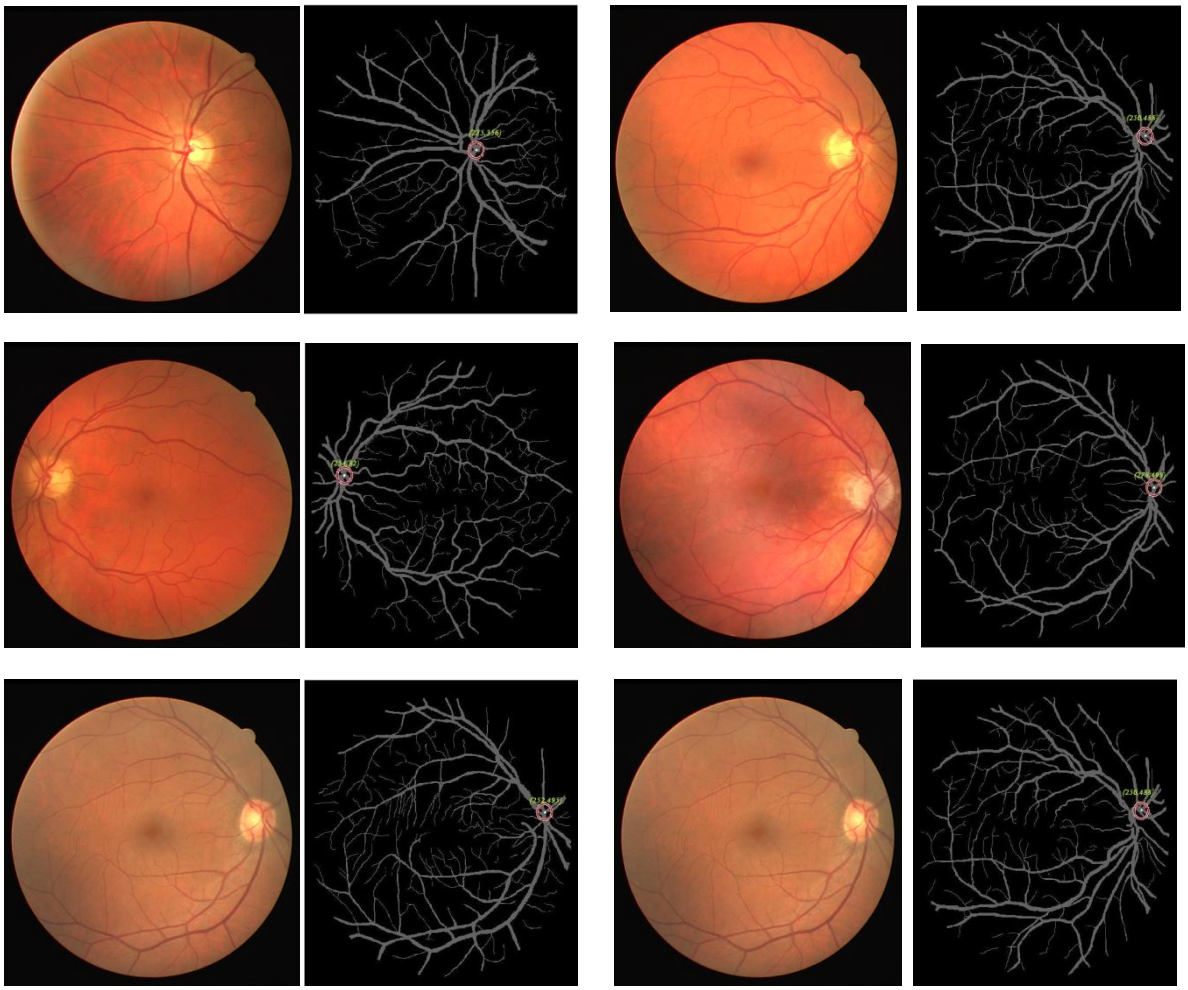

***Figure 14**:(a) original rgb image,(b)image showing OD localized on segmented image.*

4.4.3 DATABASE (CENTER OF OPTIC DISC OF THE IMAGES ON DRIVE DATABASE)

TABLE 3

image no	optic disk(X)	optic disk(Y)
1	268	80
2	250	488
3	289	82
4	275	356
5	265	67
6	277	465
7	278	498
8	258	493
9	264	77
10	267	498
11	264	58

12	275	70
13	249	507
14	283	483
15	253	212
16	274	478
17	256	474
18	249	503
19	258	486
20	268	493
21	264	54
22	255	466
23	269	424
24	287	480
25	250	469
26	249	75
27	263	495
28	250	488
29	277	506
30	281	504
31	260	367
32	286	494
33	253	365
34	264	370
35	293	75
36	250	401
37	292	503
38	250	502
39	269	82
40	282	478

4.5 CONCLUSION:

With the rapid growth of biometric authentication, searching an efficient feature is essentially important and challenging task for faster computation. So keeping the primary objectives in mind, i.e., to search a new feature for preparing a retinal template for biometric authentication and to detect the final stage of PDR, we have executed the proposed algorithm on 32 bit Matlab 2013a version on 32 bit Windows XP running on Intel Core-2 dual processor with 2 GB of RAM. The experimental results are clearly showing the detected Optic Disc location on segmented fundus image and a count on total vessels present and their distances. From the experiment, we are now able to generate a statistics on the average number of prime vessels present in a normal retina and this feature could also be applied as a new parameter in preparing retinal template in near future.

CHAPTER 5: IDENTIFICATION OF THE CENTER OF THE MACULA:

5.1 BLOCK DIAGRAM:

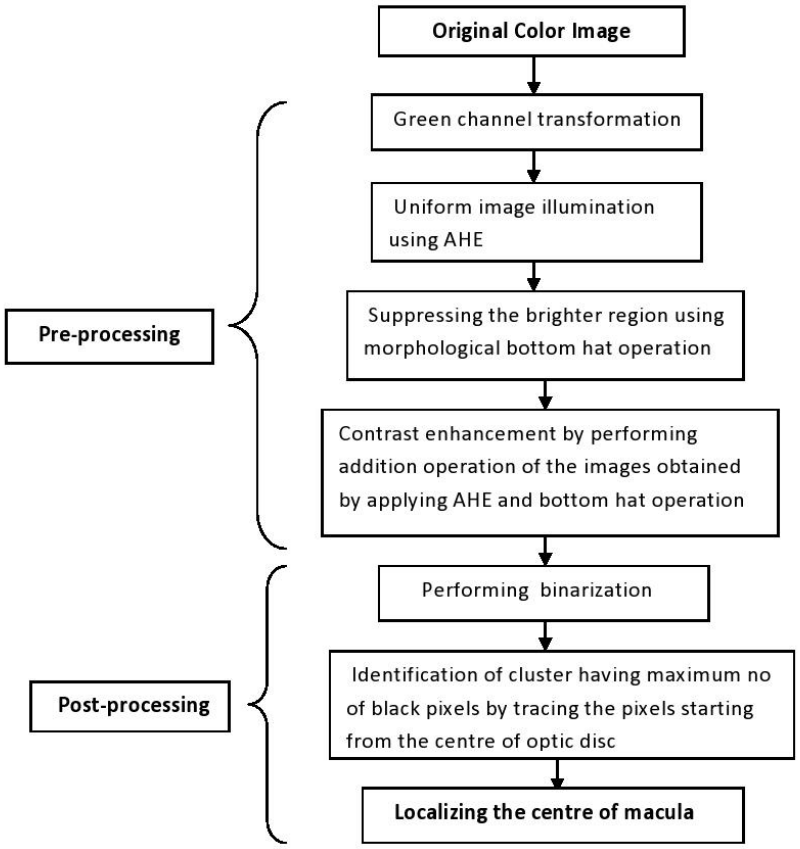

5.2 EXPLAINATION

Proposed Algorithm of localization of the macula

Proposed method of detection of macula in the color retinal image has been divided into two stages: 1)Pre-processing 2) Detection of macula .

5.2.1 Pre-processing : Pre-processing steps of the proposed algorithm has been divided into five stags

5.2.1.1 Channel Conversion:- The input image is a color (RGB) image. The red channel is the brightest color channel and has low contrast. The green channel provides the best vessel background contrast of the RGB representation. So the green channel of the image is extracted from the original RGB retinal images. Please refer Figure15.Images of the three channels and its histogram is shown in Figure16.

(a) (b) (c) (d)

Figure15*(a):original RGB image,(b)red channel image,(c)green channel image,(d)blue channel image(left to right)*

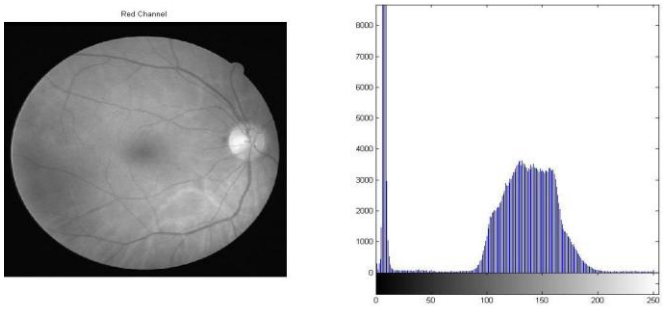

Figure 16. (*a) Red channel image and its histogram*

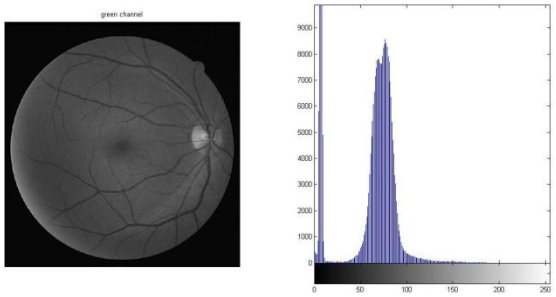

Figure16*(b) Green channel image and its histogram*

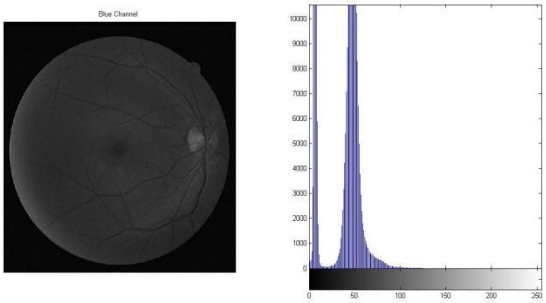

Figure16(c) *Blue channel image and its histogram*

5.2.1.2 <u>Uniform the illumination of the image</u>:- Fundus images has background intensity variation due to non uniform illumination which may deteriorate the segmentation result . Due this non uniformity in the image Background pixels may have their gray levels higher than the vessel pixels. So in this phase global thresholding techniques cannot be applied due to the various gray levels in different areas in the image and noisy unconnected regions appeared as false vessels Hence Contrast-limited adaptive histogram equalization is applied for enhancing the contrast of the green channel retinal image to redistribute the lightness value of the image .This enhancement operation is performed on the small regions of the image , instead of the entire image and thus contrast of every smaller region is enhanced .Please refer Figure 17(a) ,Figure 17(b) ,Figure 18(a) and Figure 18(b),

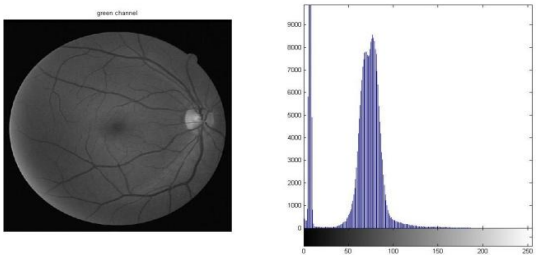

(a) (b)

Figure 17*(a): green channel image, (b) its Histogram*

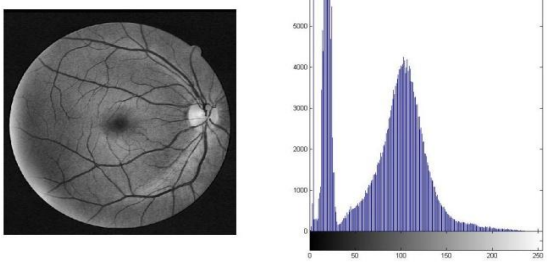

(a) (b)

Figure 18(*a) AHE filtered image (b) its histogram,*

5.2.1.3 Morphological Transformation: This pre-processing stage consists on generating a new vessel-enhanced image, which proves more suitable for further detection of macula. Vessel enhancement is performed by applying the morphological Top-Hat transformation where is a morphological opening operation using a disc of 50 pixels in radius. Thus, while bright retinal structures are removed (i.e., optic disc, possible presence of exudates or reflection artifacts), the darker structures remaining after the opening operation become enhanced (i.e., blood vessels, macula, fovea, or hemorrhages).Please refer Figure 19. The top-hat transformation is difference between an input image and its opening.

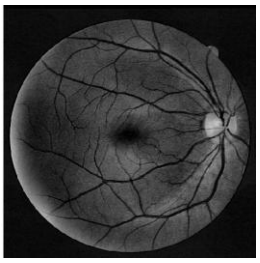

Figure 19: *image obtained after tophat operation*

5.2.1.4 Contrast enhancement: This stage increases the contrast of the image by performing addition operation of the image obtained after previous stage with the image obtained after adaptive histogram equalization. Thus, the lighter structures (background) remaining after the addition operation become enhanced. Please refer figure 20.

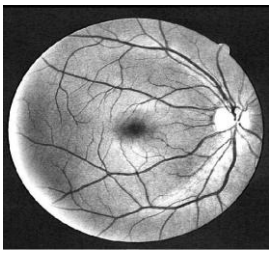

Figure 20:*image obtained after contrast enhancement*

5.2.2 Binarization of the preprocessed image: The preprocessed image is thresholded using the OTSU's method keeping the information below the threshold value and giving the rest of the image the same value as the threshold. Thus cluster based algorithm is used to perform clustering based image thresholding and the preprocessed gray scale image is reduced into the binary image. Please refer figure 21.

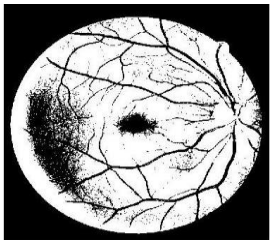

Figure 21: *image obtained after binarization.*

5.2.3 Detection of macula: After detection of the optic disc in the retinal fundus image a window of threshold size has been considered around it to remove this region from the pre-processed binary image. This will remove the false detection of the dark region nearest to the optic disc as macula. Next, from the extreme end of this rectangle towards macula, binary image Is traced horizontally upto a threshold distance towards other end along the x co-ordinate of the centre of the optic disc by considering an window of size 50X50 to find the cluster with maximum black pixels

count. After localizing this high density region, each pixel in this region is checked by considering a window of size 30X30 to find the pixel having maximum no of neighboring black pixels around it . This pixel is considered as the centre of the macula. Please refer figure 22.

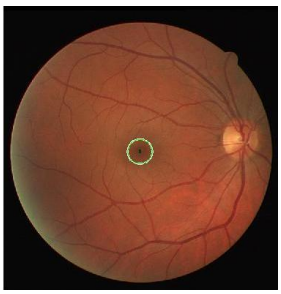

Figure 22:*image showing macula and its center after detection.*

Algorithm: Calculation of the distance between centre of optic disc and that of macula:

If the centre of optic disc is (x, y) and the centre of the macula is (s, t), then the distance between them is defined by

$$De = \sqrt{(x - s)2 + (y - t)2} \quad (2)$$

Please refer Figure 23.

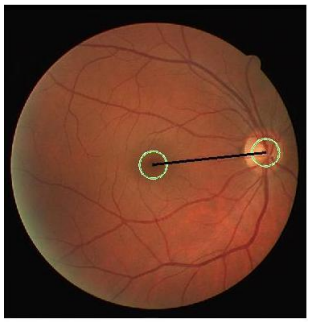

***Figure 23**. Showing the distance between macula and optic disc center*

5.3 EXPERIMENTAL RESULT AND ANALYSIS

5.3.1 EXPERIMENTAL SETUP

To evaluate the performance of the proposed system experiments have been conducted base on the DRIVE[2] and VARIA[3] database. The photographs for the DRIVE database were obtained from a diabetic retinopathy screening program in The Netherlands. Each image was captured using 8 bits per color plane at 768 by 584 pixels. For the training images, a single manual segmentation of the vasculature is available. For the test cases, two manual segmentations are available; one is used as gold standard, the other one can be used to compare computer generated segmentations with those of an independent human observer

5.3.2 RESULTS ON FUNDUS IMAGES

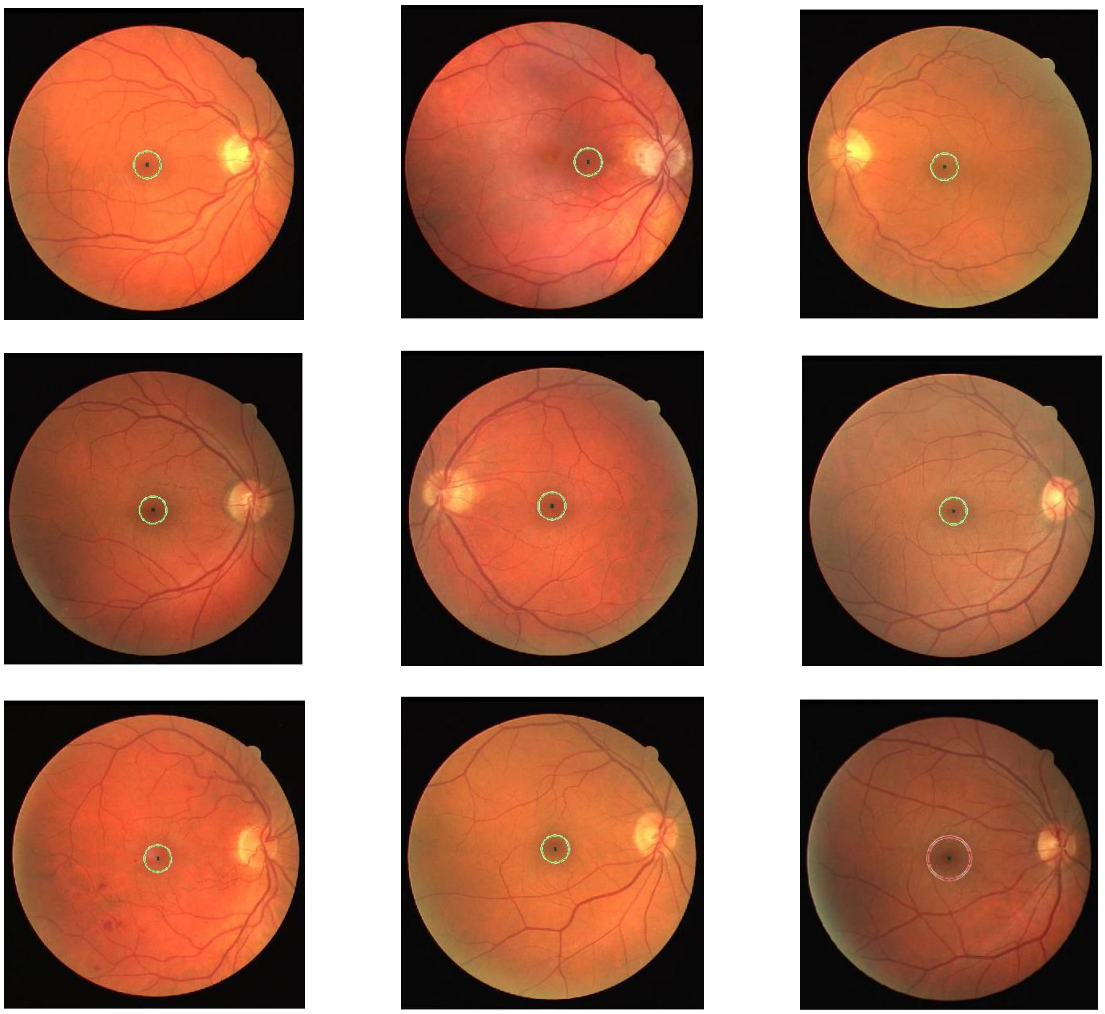

Figure 24*:image showing localized macula in original rgb image.*

5.3.3 DATABASE(CENTER OF OPTIC DISC AND MACULA AND THEIR DISTANCE)(Table 12)

Image no optic disc center macula center distance

1	(268,80)	(282,293)	203
2	(250,488)	(272,294)	220
3	(289, 82)	(291,293)	209
5	(265, 67)	(282,293)	217
6	(277, 465)	(288,294)	178
7	(278, 498)	(357,291)	140
8	(258, 493)	(286,303)	212
9	(264,77)	(282,298)	208
10	(267,498)	(285,295)	215
11	(264,58)	(281,291)	225
12	(275, 70)	(288,282)	209
13	(249, 507)	(293,285)	213
14	(283, 483)	(293,288)	199
16	(274, 478)	(285,292)	199
17	(256, 474)	(286,281)	189
18	(249, 503)	(293,286)	219
19	(258, 486)	(299,283)	207
20	(268, 493)	(300,291)	213
21	(264, 54)	(291,271)	217
22	(255, 466)	(302,282)	194
24	(287, 480)	(289,281)	200
25	(250, 469)	(298,284)	182
26	(249, 75)	(295,282)	202
27	(263, 495)	(300,280)	221
28	(250, 488)	(296,290)	198
29	(277, 506)	(301,279)	226
30	(281, 504)	(296,287)	185
32	(286, 494)	(296,282)	235
35	(293, 75)	(295,285)	210
36	(250, 461)	(296,281)	202
37	(292, 503)	(296,285)	212
38	(250, 502)	(293,287)	213
39	(269, 820)	(297,281)	193

5.4 CONCLUSION:

We have presented technique for detection of macula position in fundus images. This technique is using multilevel thresholding, contour, and ellipse detection. Proposed method was very successful on test dataset from DRIVE database (40 fundus images). Macula was successfully located on all images where was presented and we detected macula area with 90% effectivity (36 of 40).

CHAPTER6. CALCULATION OF WIDTH OF THE RETINAL BLOOD VESSELS:

6.1 BLOCK DIAGRAM

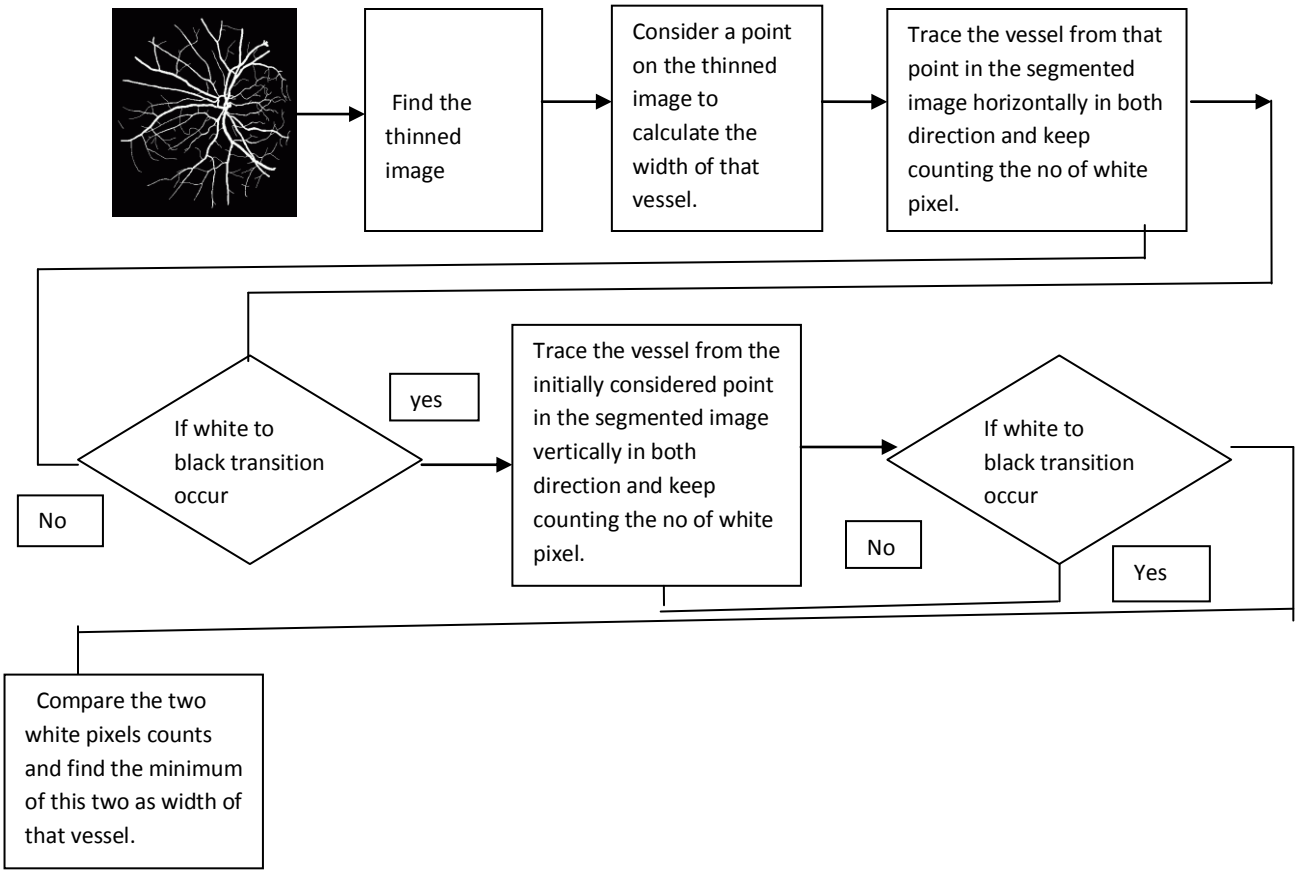

6.2 EXPLAINATION

Proposed Algorithm of width calculation of the retinal blood vessel:

The algorithm is being described over here as a cumulative.

Step 1.The algorithm starts with the segmented image as its input.

Step 2. Anatomically, there are two possible scenarios of the vessels exist which are emanating out of the Optic Disc, please refer Figure 25.

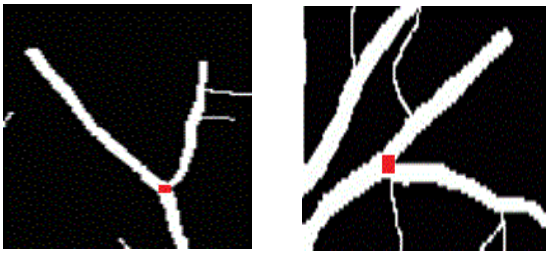

***Figure 25**: The tendency of the nerve is to move along (a) vertical direction (b) horizontal direction .*

i.e., either they tend to move along the horizontal direction, or they are prone to the vertical direction.

So, to measure the width of any vessel at any point, careful steps has been taken about the directions and this could be done unerringly by comparing the number of white pixels along the vertical direction with the number of white pixel in the horizontal one. Then the minimum count of these two will be considered as the width of the present vessels at that point. Hence to calculate the width of the vessel first of all we are taking the thinned image of the original segmented image and then a point on the vessel at a certain distance around the optic disc in the thinned image is taken. For a single point on every nerves around the optic disc following steps are applied.

Step 2.1. Start tracing the vessel horizontally by counting the number of white pixel until a transition takes place from white to black pixel. The same process is repeated for both the left and right directions from that point in the original segmented image, see figure 26(a).

Step 2.2. Then, vertical tracing is done again by counting number of white pixels until a transition takes place from white to black pixel. The process continues for both the upward and downward directions from that point in the original segmented image. Please refer see figure 26(b).

Step 2.3. Then, the minimum count between horizontal and vertical directions is being selected as the width of the specified vessel .

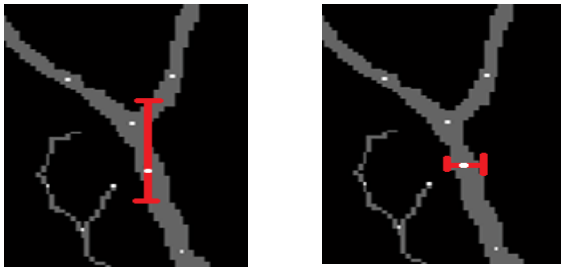

***Figure 26**:Comparing this two count and as count along vertical direction count along horizontal direction hence we can predict that tendency of the nerve is along the vertical direction .so the width of the nerve at that point is equal to the count along the horizontal direction (a) Counting the no of pixel While moving along the vertical direction i.e. upward and downward direction from the point (b) Counting the no of pixel While moving along the horizontal direction i.e. along left and right from the point .*

6.3 Complexity Analysis:

While calculating the width of the vessel ,we are moving in left and right direction horizontally until a white to black transition occur and similarly in vertical directions also . Both the cases , it consumes linear amount of time , i.e., the above algorithm results into a time complexity of O(n). Apart from this there would be obvious need of O(n2) amount of time while scanning the entire image for processing. And as there is no additional space or storage are required, we conclude the space complexity as constant.

6.4 CALCULATION OF RATIO OF WIDTH OF CHILD VESSELS TO THE WIDTH OF THE PARENT VESSEL

6.4.1 ALGORITHM

```
Ensure:
nv ← number of pixels in vertical direction
nh ← number of pixels in horizontal direction
nv ← 0
nh ← 0
width ← total width of vessel
width ← 0
parent ← width of the parent vessel
child1 ← width of one child vessel
child2 ← width of another child vessel
 for each bifurcation point do mark three distinct point on the three branches around it
       for each of these points on the respective three branches do
           repeat move along the upward vertical direction
           nv ← nv + 1
           and move along the downward vertical direction also
           nv ← nv + 1
           until white to black transitions occur

          repeat move along the left horizontal direction
          nh ← nh + 1
          and move along the right horizontal direction
          nh ← nh + 1
          until white to black transitions occur
         if nv > nh then
            width :← nh
        else
           width :← nv
        end if
     end for
      calculate ratio1 :← parent/child1
      calculate ratio2 :← parent/child2
end for
```

6.4.2 EXPLANATION

The bifurcation points ensure stability and are not subject to any change even when prone to diseases. Identifying these points, our algorithm attempts to find the ratio of the width of a parent vessel with its corresponding child vessels at the bifurcation points. Experimental results prove that this ratio lies in the range of 1.1-1.8

6.4.3EXPERIMENTAL RESULT

DATABASE (RATIO OF THE NO OF PARENT NERVES TO THE CHILD NERVES for image no 4 in drive database)

Table 4

Image No.	Location(X,Y)	Parent width	Child1 width	child2 width	Parent:child1	Parent:child2
4	51 , 285	9	3	8	3	1.125
	61 ,398	7	4	3	1.75	2.333333
	72 , 399	11	9	11	1.222222	1
	77, 260	4	3	3	1.333333	1.333333
	96 , 322	8	6	7	1.333333	1.142857
	101 , 418	4	3	3	1.333333	1.333333
	102 ,419	4	4	4	1	1
	103 ,418	4	3	4	1.333333	1
	104 ,473	5	5	3	1	1.666667
	106 ,137	6	4	5	1.5	1.2
	112 ,442	10	7	4	1.428571	2.5
	118 ,476	9	3	4	3	2.25
	119 ,355	4	3	3	1.333333	1.333333
	120 ,476	10	5	10	2	1
	130 ,312	3	3	3	1	1
	131 ,417	10	4	9	2.5	1.111111
	143 ,441	20	5	10	4	2
	151 ,342	9	3	7	3	1.285714
	159 ,101	10	8	3	1.25	3.333333
	166 ,478	7	6	3	1.166667	2.333333
	174 ,145	9	7	8	1.285714	1.125
	175 ,362	14	10	11	1.4	1.272727
	184 ,511	13	3	6	4.333333	2.166667
	190 ,196	10	6	8	1.666667	1.25
	192 ,380	13	9	10	1.444444	1.3
	199 ,522	8	4	4	2	2
	205 ,301	9	6	7	1.5	1.285714
	215 ,437	5	3	3	1.666667	1.666667
	217 ,367	12	3	10	4	1.2
	219 ,347	10	4	4	2.5	2.5
	221 ,347	14	9	14	1.555556	1
	221 ,463	4	3	4	1.333333	1
	225 ,467	4	4	4	1	1
	229 ,194	8	8	3	1	2.666667
	239 ,391	5	4	3	1.25	1.666667
	240 ,290	10	3	9	3.333333	1.111111
	243 ,475	7	3	3	2.333333	2.333333
	244 ,432	3	3	3	1	1

6.5 COMPUTATION OF TOTAL NO OF MAJOR BLOOD VESSELS

6.5.1 ALGORITHM: COUNTING NUMBER OF BLOOD VESSELS AROUND OPTIC DISC

```
Ensure
  count <− total number of blood vessels around optic disc
  consider a 50x50 window around the optic disc
  repeat
  for each pixel along the window border
    if a white pixel is found then
      repeat
        move along the border of the window by one pixel
      until white to black transition occur
      count <− count+1
   else
      move along the border of the window by one pixel
   end if
 end for
until all the pixels along the four border of the specified window is traversed
```

6.5.2 EXPLANATION

Different parameters like accuracy, specificity, sensitivity are defined in order to compare the results from the algorithm with the segmentation of other algorithms. To compute this parameters one of the fundamental steps is calculating number of blood vessels detected by the algorithm so that it can be compared with the gold standard images. Moreover counting no of blood vessels around optic disc helps in diagnosis of PDR. Hence counting number of blood vessels around the optic disc would serve our purpose. Please refer Algorithm 2 for counting number of blood vessels around the optic disc and table 1 for the number of blood vessels detected by the algorithm applied on the DRIVE database.

6.5.3 EXPERIMENTAL RESULT AND ANALYSIS

6.5.3.1 EXPERIMENTAL SETUP

To evaluate the performance of the proposed system experiments have been conducted base on the DRIVE[2] and VARIA[3] database. The photographs for the DRIVE database were obtained from a diabetic retinopathy screening program in The Netherlands. Each image was captured using 8 bits per color plane at 768 by 584 pixels. For the training images, a single manual segmentation of the vasculature is available. For the test cases, two manual segmentations are available; one is used as gold standard, the other one can be used to compare computer generated segmentations with those of an independent human observer. The VARIA database is a set of retinal images used for authentication purposes. The database currently includes 233 images, from 139 different individuals. The images are optic disc centered with a resolution of 768x584[3].

6.5.3.2 RESULTS OF NO OF MAJOR BLOOD VESSELS AROUND THE OPTIC DISC

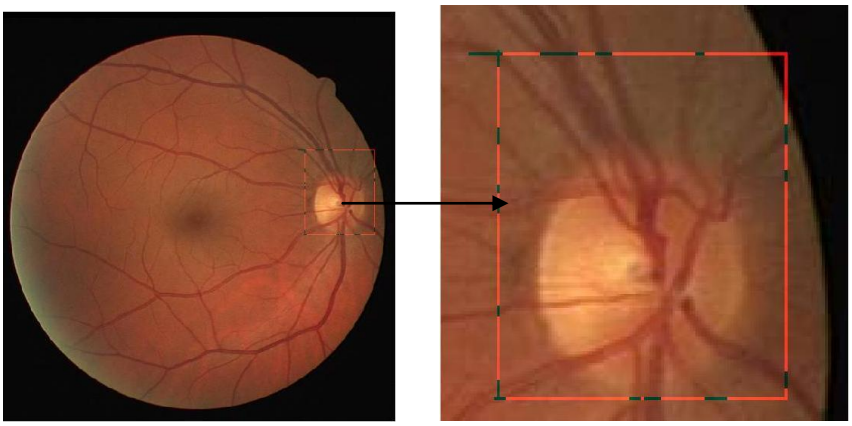

Figure 27 *images showing the major blood vessels around the optic disc and distance between each consecutive blood vessels(vessel width is shown by green line and distance between the vessels is show by red line)*

6.5.3.3 DATABASE (NO OF MAJOR BLOOD VESSELS AROUND OPTIC DISC APPLIED ON THE IMAGES OF DRIVE DATABASE)

6.5.3.3.1 VARIA DATABASE (Table 5)

Imageno	X	Y	Total Vessel	Total Distance
1	258	465	8	201
2	272	565	8	167
3	327	543	7	192
4	313	442	8	190
6	255	543	8	247
7	289	488	6	217
9	260	457	9	239
11	265	451	6	193
13	279	458	11	169
14	303	548	7	150
16	275	474	4	129
18	264	583	7	133
19	300	597	8	157
20	304	515	8	213
22	267	524	8	193
23	296	535	6	191
25	257	533	5	161
26	264	458	8	207
27	288	522	6	210
28	249	515	9	167
29	264	504	7	216
33	247	507	6	197
34	309	466	7	251

35	313	475	9	237
36	259	500	8	161
38	288	594	9	153
39	263	544	8	202
40	304	468	11	244
41	282	584	7	140
42	250	400	10	255
43	260	525	6	180
45	302	446	11	239
48	260	465	9	253
49	263	545	8	239
50	291	548	4	189

6.5.3.3.2 DRIVE DATABASE (Table 6)

Image no	Optic disc(X)	Optic disc(Y)	vessel count	vessel distance
1	268	80	14	185
2	250	488	12	170
3	289	82	16	157
4	275	356	13	189
5	265	67	12	174
6	277	465	12	184
7	278	498	16	185
8	258	493	16	170
9	264	77	14	187
10	267	498	13	153
11	264	58	10	155
12	275	70	12	183
13	249	507	10	172
14	283	483	13	175
15	253	212	12	174
16	274	478	12	171
17	256	474	13	167
18	249	503	10	163
19	258	486	11	172
20	268	493	11	177
21	264	54	11	174
22	255	466	13	168
23	269	424	14	185
24	287	480	10	182

6.6 DISTANCES BETWEEN TWO CONSECUTIVE BLOOD VESSELS AROUND OPTIC DISC

Distance between the consecutive blood vessels is measured which helps in identification of PDR at very earlier stage. an odd sized window around it is fixed keeping the center pixel of the window as the detected Optic Disc. While scanning this window clockwise, the vessel locations are pointed and a counter is getting increased to keep track of the number of vessels. Then the distance between each consecutive vessels are calculated by Euclidean Distance measurement.

If the initial location is (x,y) and final points are (s,t), then the distance between them is defined by

$$De=\sqrt{(x-s)^2 + (y-t)^2} \quad (3)$$

Total distance is again a cumulative distance of all the vessels emanating out from the OD.
It is defined by

$$\text{Total distance} = \sum_{i=1}^{n} vessels_I \quad (4)$$

Where n is the maximum number of blood vessels.

6.6.1 EXPERIMENTAL RESULTS

6.6.1.1 VESSEL WIDTH AROUND THE OPTIC DISC (DRIVE DATABASE):

TABLE 7

img	w1	w2	w3	w4	w5	w6	w7	w8	w9	w10
1	3	4	7	9	12	6	2	2	3	4
2	2	5	11	10	6	6	6	5	8	6
3	5	7	5	4	3	11	9	2	22	2
5	7	3	10	16	5	4	3	3	7	8
6	2	4	3	8	16	3	1	11	10	6

6.6.1.2 (VARIA DATABASE) VESSEL WIDTH AROUND THE OPTIC DISC

TABLE 8

img no	w1	w2	w3	w4	w5	w6	w7	w8	w9	w10	w11	w12	w13	w14
1	8	11	12	8	14	2	1	1						
3	3	5	2	5	2	12	4	3	16					
6	4	10	6	3	9	8	6	12	7					
9	7	11	5	12	13	9	12	15	26					
13	1	5	11	14	11	9	1	6	20	7	4	15	12	4
14	5	15	7	5	13	9	7	3						
19	2	7	3	8	8	15	10	8	7					

*** w stands for width of a vessel**

6.6.3.1 DISTANCE BETWEEN THE VESSELS AROUND OD(DRIVE DATABASE)

TABLE 13

Image No.	Total nerv	D1	D2	D3	D4	D5	D6	D7	D8	D9	D10	D11	D12	D13	D14
1	13	15	16	2	39	4	62	6	13	6	18	11	4	3	8
2	12	7	17	1	5	34	7	21	5	36	13	21	37		
3	16	4	17	12	5	12	7	12	7	7	1	14	5	9	17
4	13	24	42	6	9	49	23	18	6	11	17	12	13	5	
5	10	27	17	4	2	22	17	24	17	11	16				
6	12	10	21	25	16	3	32	11	16	14	10	10	30		
7	16	7	11	6	13	5	18	3	24	31	13	15	4	24	5
8	16	14	19	5	25	2	10	4	22	2	9	7	3	4	15
9	14	25	11	3	7	22	3	11	5	29	9	9	16	12	17
10	13	7	6	1	4	4	15	36	20	1	19	5	23	9	
11	10	33	2	7	9	7	22	8	23	7	9				
12	12	32	15	17	7	14	25	16	5	12	15	12	11		
13	14	13	13	18	8	6	13	2	19	12	21	1	20		
14	13	28	3	26	3	2	4	7	17	23	7	7	15	40	
15	12	15	7	19	12	1	39	18	3	28	16	15	8		
16	14	37	10	6	5	3	14	7	3	38	27	7	5	21	16
17	13	24	5	1	21	5	14	24	2	8	10	20	5	35	
18	9	46	19	3	51	5	13	15	7	17					
19															
20	7	18	16	38	17	2	6	48							
21	11	25	21	19	11	11	15	21	6	10	15	29			
22	13	21	19	2	33	2	3	4	8	20	13	22	24	6	
23	13	9	10	37	5	24	8	11	6	19	6	3	18	19	
24	10	9	21	28	13	23	10	8	24	25	10				
25	12	11	14	13	1	8	24	11	3	25	28	8	37		
26	11	9	20	6	11	64	2	30	22	9	15	31			
27	14	25	7	10	5	1	8	15	15	7	21	14	8	19	12
28	11	3	30	4	22	8	1	11	35	4	25	16			
29	10	33	2	22	2	18	29	16	15	7	21				
30	10	27	18	2	30	42	14	14	6	5	24				
31	13	3	10	12	12	14	17	3	11	14	16	6	11	29	
32	13	19	4	8	20	3	28	30	25	14	19	8	6	3	
35	15	9	21	2	18	33	4	34	1	18	11				
36	8	20	26	11	21	41	18	9	32						
37	10	12	27	18	4	27	26	25	4	26	32				
38	12	15	16	9	9	17	2	14	4	46	16	23	44		
39	12	23	26	3	5	9	14	15	38	6	7	22	18	10	
40	10	18	20	11	7	15	11	44	11	26	33				

6.7 DETECTION OF PROLIFARATIVE DIABETICS RETINOPATHY (PDR)

Additionally, biometric template based on this feature would be robust enough to fight against even the situation of Proliferative Diabetic Retinopathy (PDR) where newly generated, tiny fragile vessels interrupt the authentication process. At the advanced stage of Proliferative Diabetic Retinopathy, signal sent by the retina triggers the development of new fragile blood vessels that proliferate in the retina and the vitreous, which is a transparent gel that fills the interior of the eye please refer Figure28. As these new vessels are not normal in nature, they can rupture and bleed, causing hemorrhages in the retina or vitreous. Scar tissue can develop and can tug at the retina, causing further damage or even retinal detachment .This algorithm can be used to find the width of the vessel around the optic disc which may be intended in diagnosing of PDR. Lot of variations in the width of the blood vessels around optic disc indicates the probability of generation of fragile nerves due to PDR.

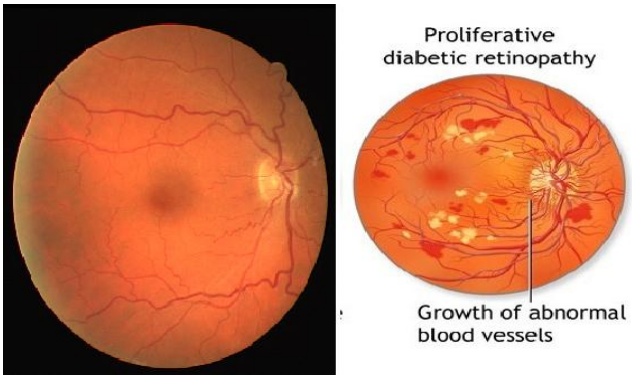

(a) (b)

Figure28*: (a) normal retinal image (b) retinal image effected due to PDR*

6.8 CONCLUSION:

With the objective of Diagnosis of Proliferative Diabetic Retinopathy in its early stage by separating the newly generated fragile tiny vessels with the original ones and detection of any abnormality in the fundus image in mind, we have executed the proposed algorithm on 32 bit Matlab R2013a version on 32 bit Windows 7 running on Intel Core2 dual processor with 2 GB RAM. Experimental results show the width of individual major vessels around the Optic Disc and throughout the whole image. Additionally, from the experimental result we have found that the ratio of each parent to child vessels at every bifurcation point is within the range of 1.1 to 1.8. Also, for the images which are severely a ected by the nal stage of PDR, this method would be able to diagnose them effortlessly by keeping track width of the vessels around the optic disc. We hope this work would be worthwhile for the ophthalmologists also in analyzing the retinal images to diagnose PDR even at the initial stage.

CHAPTER 7: IDENTIFICATION OF DISTINCT BIFURCATION AND CROSSOVER POINTS AND BIFURCATION ANGLES

7.1 IDENTIFICATION OF DISTINCT BIFURCATION AND CROSSOVER POINTS

7.1.1 BLOCK DIAGRAM:

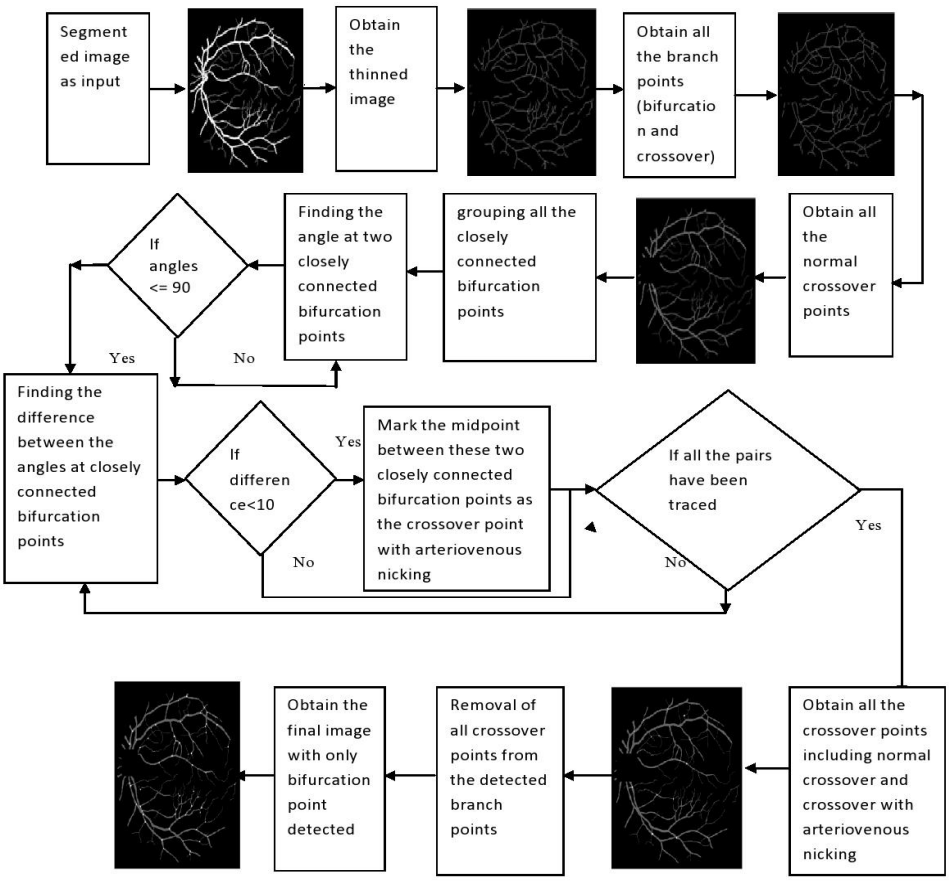

7.1.2 ALGORITHM

Algorithm 1 Bifurcation point calculation

Ensure:
points ← detected branch points bifurcation
points ← detected bifurcation points
diff ← difference between the angles at two close bifurcation points do skeletonization of the segmented image
for each detected branch points
do count the no of neighboring pixels including the chosen one by considering a small rectangular window surrounding it
if count == 5 then
mark the branch point as normal crossover and remove the point from detected branch points
end if
end for

find the closely connected bifurcation points from the remaining detected branch points and group them individually
for each detected closely connected bifurcation pair
do find the angle at two close bifurcation points and mark as 1 and 2
if $\alpha 1 < 90$ and $\alpha 2 < 90$ then
diff = abs($\alpha 1 - \alpha 2$)
else if diff <= 10 then
mark the midpoint of the two closely connected bifurcation points generated due to arteriovenous nicking as a single crossover that is represented by two closely connected bifurcation points in the skeleton image
end if
end for

7.1.3 EXPLAINATION

Proposed algorithm of identification of distinct bifurcation points:

Step 1. This algorithm starts with the segmented images from DRIVE database as its input.

Step 2. The segmented images are being thinned by using a standard morpho- logical thinning function of Matlab. Then all the branch points of the thinned images are calculated using another morphological function 'bwmorph' along with the operation branchpoints'. The term branch point includes both the bi- furcation and the crossover points.

Step 2.1. These crossover points are basically of two categories, one is the normal one and another is a false situation which is often detected as bifur- cation point due to arteriovenous nicking occurs at the crossover points. Please refer the figure 3.

Step 3. Next, all the crossover points are needed here to be removed using the following steps.

Step 3.1. A $3 * 3$ window is being considered to traverse around each selected branch point. The window is then scanned to find out the total number of neighborhood white pixels surrounding the branch point.

Step 3.2. If this count gives a number which is equal to a predefined threshold value five including that branch point pixel, this pixel is marked as a normal crossover point then. At the end, all the normal cross over points have been successfully detected as shown in the following figure 29.

Step 3.3. The term arteriovenous is the junction where two very close

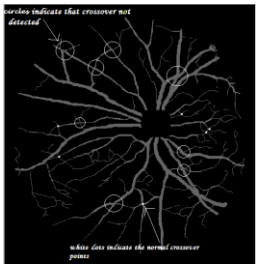

Figure29 *Detected normal crossover points vessels meet and creates a troublesome situation.*

This exceptional situation of- ten arises in the skeleton image and always there is a common probable scenario to identify this junction as two very close bifurcation points together. However, this process may lead to a false detection of real scenario as two bifurcation points also as shown the figure 30 where the two bifurcation points are really close in nature. With a hope to get a better solution here and to differentiate between true crossovers from

spurious results, another geometrical features of each detected crossover are analyzed along with notion of two closely connected bifurcation points.

Step 3.3.1. The intersection angles formed by the two vessels at the crossing are a1 and a2 shown in the following figure 31.

Step 3.3.2. Then all the closed bifurcation points are detected and grouped together.

Step 3.3.3. Finally, for each group of two closely connected bifurcation points, the bifurcation angles are calculated as α1 and α2. It has been

Figure. 30 *Showing arteriovenous nicking*

observed that when a crossover appears as two closed bifurcation points in the skeleton image due to the thinning process, the two angles formed by the two segments i.e. vessels associated with each bifurcation point represent the acute angles of the intersection. Hence, α1 and α2 values of a true crossover should be less than a certain threshold. And also from statistical analysis it has been found that if the difference between α1 and α2 are less than a predefined threshold 10, then this two closed bifurcation points can be considered as a single crossover point.

error:=difference between α1 and α2 =(α1 -α2) if(error<= 10) then two closed bifurcation points is detected as a single crossover point. then, mid point of these two closed bifurcation points is considered as a single crossover point as shown in the following figure 32.

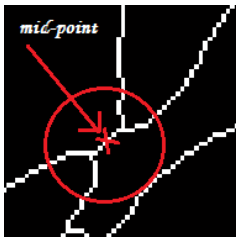

Figure. 31. *Mid point of two closely connected bifurcation points detected as a single crossover point*

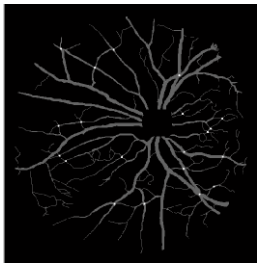

Figure. 32 *All the crossover points detected through the above steps*

Step 4. Then the result sets are found after the crossover points has been detected. In the evaluation process, all crossovers which fall within the optic disk are excluded from evaluation. In addition, the very small tiny vessels may cause some errors while calculating the no of crossover points from a fundus image which are negligible.

7.1.4 EXPERIMENTAL RESULT AND ANALYSIS

7.1.4.1 EXPERIMENTAL SETUP

To evaluate the performance of the proposed system experiments have been conducted base on the DRIVE[2] and VARIA[3] database. The photographs for the DRIVE database were obtained from a diabetic retinopathy screening program in The Netherlands. Each image was captured using 8 bits per color plane at 768 by 584 pixels. For the training images, a single manual segmentation of the vasculature is available. For the test cases, two manual segmentations are available; one is used as gold standard, the other one can be used to compare computer generated segmentations with those of an independent human observer. The VARIA database is a set of retinal images used for authentication purposes. The database currently includes 233 images, from 139 different individuals. The images are optic disc centered with a resolution of 768x584[3].

7.1.4.2 RESULT ON DRIVE FUNDUS IMAGES

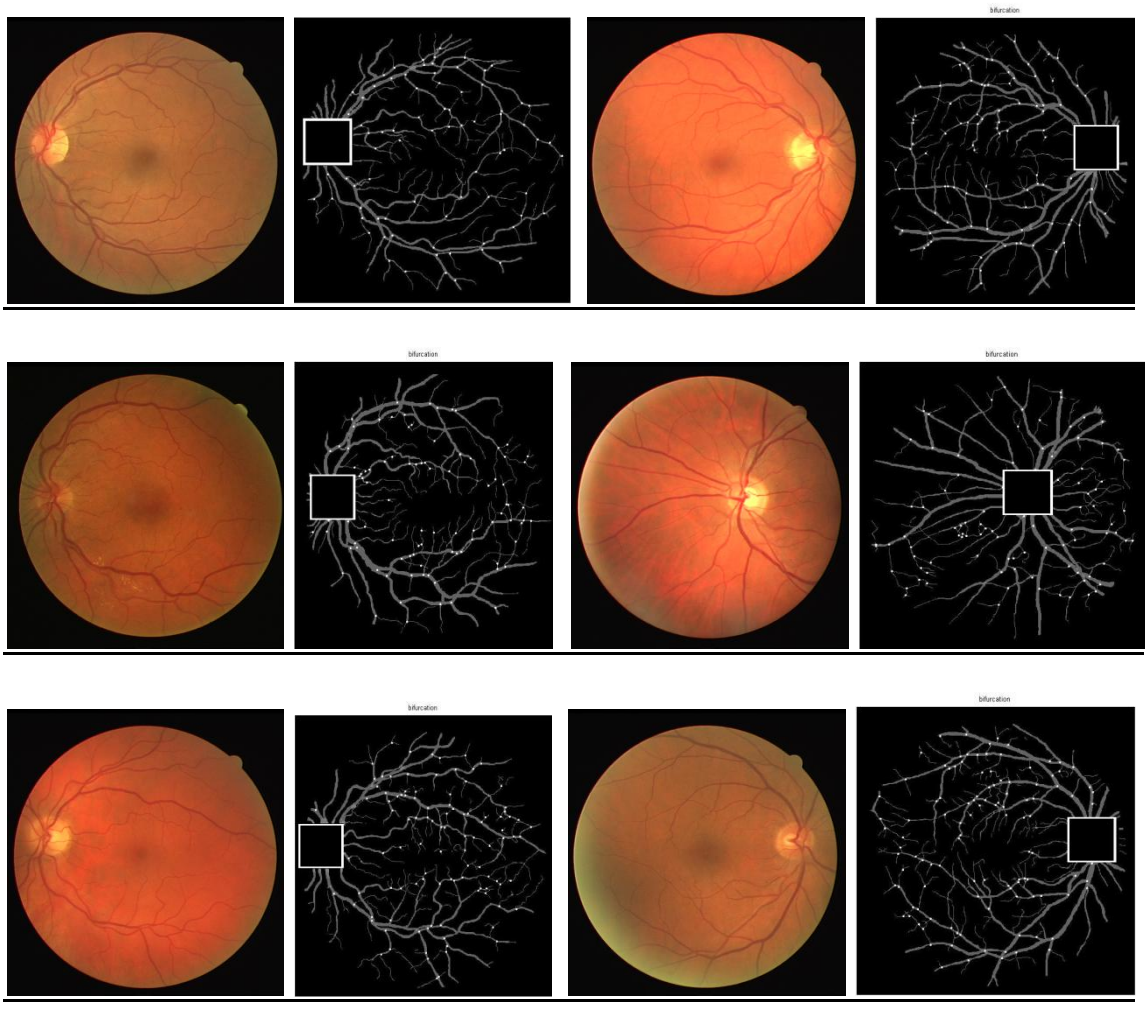

(a) **(b)** **(a)** **(b)**

Figure:33 *(a) original rgb image,(b) image showing bifurcation point detected*

7.1.4.3 PERFORMANCE EVALUATION METRIC

7.1.4.3.1 **Evaluation Parameter:** To evaluate the proposed algorithm manually following parameters are defined in order to compare the results from the algorithm with other algorithms.

- **TP (true positive):** This refers to the pixels of the blood vessels that are correctly recognized by the algorithm. Let TP denotes the number of true positives.
- **FP (false positive)**: This refers to the pixels of the blood vessels that are incorrectly recognized as positive pixels by the algorithm. Let FP denotes the number of false positive.
- **TN (true negative)**: This refers to the pixels of the blood vessels that are correctly discarded by the algorithm. Let TN denotes the number of true negative.
- **FN (false negative)**: This refers to the positive pixels of the blood vessels that were mislabeled as negative pixels by the proposed algorithm. Let FN denotes the number of false negative.

TPR, FPR, TNR and FNR are the other parameters which are also used in evaluation process are defined as follows.

- **TPR (true positive rate):** It is the ratio of the true positives to all pixels belonging to blood vessels. This is also called **SENSITIVITY.**

  Sensitivity = (Number of true positive)/ (Number of true positives + Number of false negative)
  = TP/P
  = (TP)/ (TP+FN) (4)

- **TNR (true negative rate):** It is the ratio of the false positives to all the pixels that do not belong to the blood vessels. This is also known as **SPECIFICITY**.

  Specificity = (Number of true negatives)/ **(**Number of true negatives **+** Number of false positives)
  = TN/N
  = (TN)/ (TN+FP) (5)

- **FPR (false positive rate):** It is the ratio of false positive to all the pixels that do not belong to the blood vessels. This is also known as fall-out.

  Fall-out = (Number of false positive)/ **(**Number of true negatives **+** Number of false positives)
  = FP/N
  = FP/ (TN+FP) (6)

- **FNR (false negative rate): It is t**he ratio of false negative to all the pixels belonging to the blood vessels.

  FNR = (Number of false negative)/ (Number of true positives + Number of false negative)
  = FN/P
  = FN/ (TP+FN) (7)

  Using the above parameters, accuracy of the proposed algorithm has been calculated.

- **Accuracy:** it is a description of systematic errors, a measure of statistical bias. Accuracy of the algorithm is defined as

  Accuracy (ACC) = (∑True Positive + ∑True Negative)/Total population
  = (TP + TN)/ (TP + FN + TN + FP) (8)

7.1.4.3.2 PROPOSED METHOD (TABLE 9)

Parameters	Image 12	Image 26	Image 19	Image 3
Actual bifurcations present	73	64	42	84
Detected bifurcation points	75	63	42	83
Correctly detected points	73	63	41	83
Bifurcation points not detected	0	1	1	1
Incorrect	2	0	0	0
Sensitivity	1	1	.976	.988
Specificity	0	0	0	0
Acuuracy	97.33%	98.41%	97.6%	98.8%

7.1.4.3.3 OVERALL PERFORMANCE OF BIFURCATION POINT DETECTION ALGORITHM(TABLE 10)

Database	Sensitivity	Specificity	ROC	Accuracy
DRIVE	0.98	0	0.9882	98.8%

7.2 CALCULATION OF BIFURCATION ANGLE:

7.2.1 BLOCK DIAGRAM:

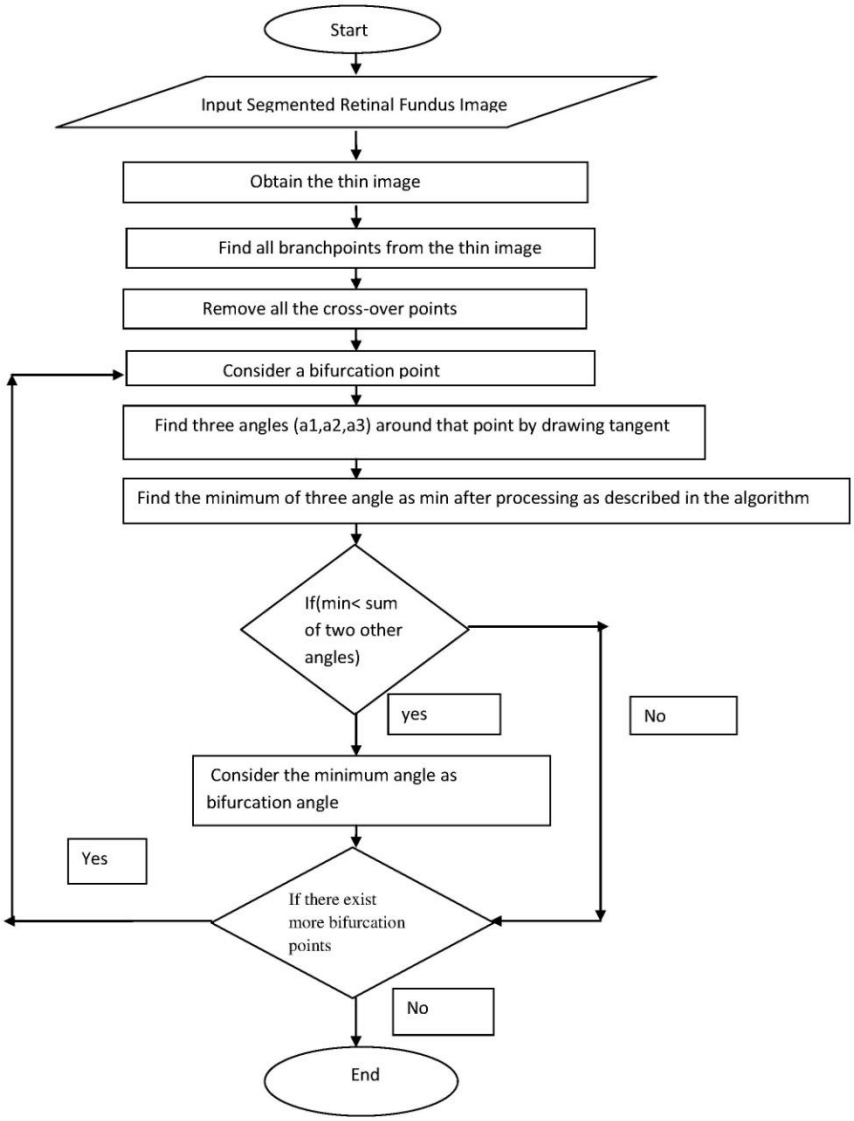

7.2.2 EXPLANATION

Objective : is to find out the three angle around each bifurcation point on the segmented input image and specifically the bifurcation angle.

Segmented image was taken as input image. All the branchpoints were found out from the segmented image using matlab defined function bwmorph with operation 'branchpoint' after morphological thinning operation has been performed on the segmented input image.

In the next step, all crossover points including false crossover points from previously found branchpoints were removed .

Hence only the bifurcation points have been almost correctly obtained from the input image. In the next step, three angle around each bifurcation points were calculated using the following steps: For each bifurcation point, in order to find three angle it is required to draw three tangent one along parent nerve and other two along the child nerve respectively. Now, in order to draw three tangents , three points one on the parent nerve and other two on the child nerve are found out respectively using the following steps:

Steps :

Thinnned image of the input segmented image was obtained with the help of matlab defined function bwmorph with the operation 'thinning'.

Around each bifurcation point , in the thinned image a 3X3 window is taken and whenever a white pixel is found , that pixel is being made as the current pixel to find the next neighborhood pixel , at the same time the previously traversed pixel in the thinned image is removed to indicate that this pixel has been traversed. This process is repeated until 18 pixel from the bifurcation point has been traversed for both three branches. Result will give one distinct point on each of the parent nerve and both the child nerves generated from the bifurcation point.

Thus, three distinct point were found out and three tangent were drawn along the three branches using the formulae

$$m=\tan\theta=(y1-y2)/(x1-x2)$$

where (x1,y1) is the bifurcation point and (x2,y2) is one of the three point found by the previous algorithm and m is the gradient of the tangent.

Then the angle between three angle were calculated using the formulae θ=tan-inverse(m1-m2)/(1+m1*m2) where θ is the angle of two tangent,m1 and m2 are the gradient of two tangent respectively.

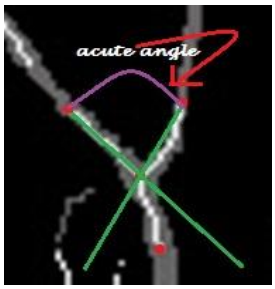

Here bifurcation angle calculated through the above formulae is an acute angle as shown in the figure . hence we get the exact value of the bifurcation angle because the angle is not distorted.

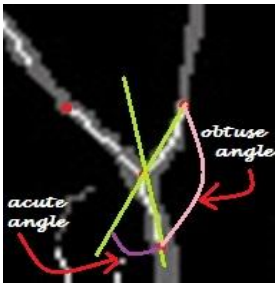

As the angle between the parent nerve and one of the child nerve which is found by the above formulae is an acute angle(shown by purple color). But the corresponding obtuse angle i.e. (180-acute angle))(as shown in the figure by pink color)will be the exact angle between these two nerve.

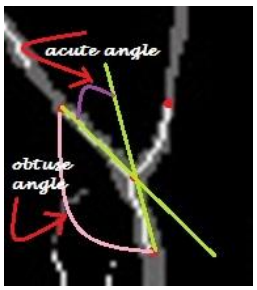

As the angle between the parent nerve and one of the child nerve which is found by the above formulae is an acute angle(as shown by purple color). But the corresponding obtuse angle i.e. (180-acute angle)(as shown in the figure by pink color) will be the exact angle between these two vessel

Hence, by using above formulae for finding the angle, three acute angles will be always obtained such that bifurcation angle will be > other two angle as shown in the figure .hence first of all the absolute value of the three angles were calculated .Then the maximum acute angle was considered as the bifurcation point(θ1). Next for other

two angles , say θ2 and θ3 corresponding obtuse angles are found i.e. Θ2=180-θ2 and Θ3=180-θ3. Hence the minimum of these three angle is the bifurcation angle and it satisfies the rule i.e. (θ1<θ2+θ3)

7.2.3 FOR DISTORTED BIFURCATION ANGLE:

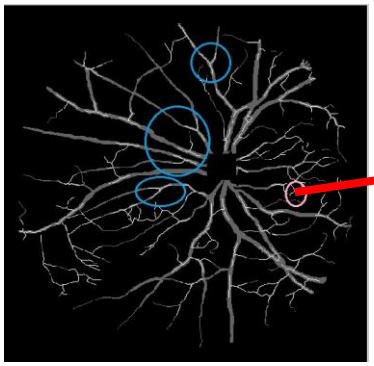

value of the bifurcation angle is calculated by the above formulae will be the acute angle (shown by purple color in the figure5) between the two child nerve. Now sum of the three angles (θ1+θ2+θ3) which are calculated by the above procedure (as shown in the figure : 6 with maroon color) is not equal 360 . hence we can conclude that it is a distorted bifurcation point .

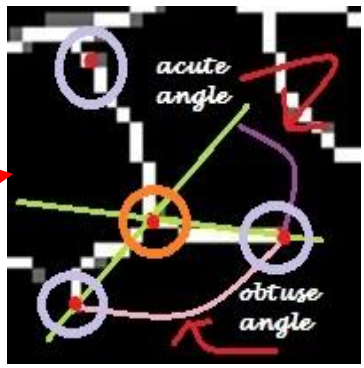

(θ1+θ2+θ3) <360

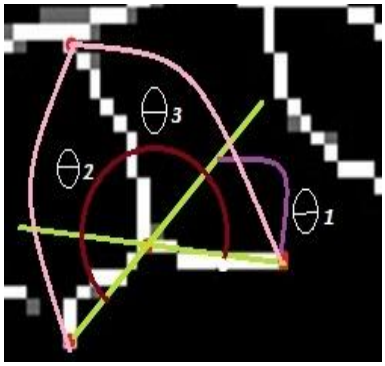

Since, it is a distorted bifurcation point(i.e. bifurcation angle >90) as shown in figure 6 , in order to find out the exact bifurcation angle corresponding obtuse angle(as shown in the figure:5) between two child nerve is to be taken i.e. (180-acute angle)

Hence, according to the previous analysis sum of the three angle(θ1+θ2+θ3) is not equal to 360 then it indicate that the bifurcation angle which was taken by the previous process is an acute angle , but in real corresponding obtuse angle is the exact bifurcation angle . Distortion in bifurcation point causes the above scenario as shown in figure . hence 180-(bifurcation angle found previously) will be the actual bifurcation angle. Hence the minimum of these three angle is the bifurcation angle and it satisfies the rule i.e. (θ1<θ2+θ3).This bifurcation points can be recognized as distorted bifurcation too.

7.3: CONCLUSION:

Detection of only bifurcation points in a fundus image is a challenging task in true sense. The purpose of the work aims to avoid numerous unnecessary hazards of appraising crossover points as one of the crucial feature for authentication. Most of the literature show the crossovers as their reliable authentication parameter. But in contrary, image capturing should always be from a fixed location and angle to avoid non-identification of the authentic source. Moreover, the patients suffering from diseases like hypertension, cardiovascular diseases and type II diabetes, often experience the change in crossover points of their retina which further increases the possibility of True Negative(TN) factor in authentication process. So to focus on only bifurcation point which is anatomically stable and never changes [14],[11], is an important issue. We have tried to accomplish this work successfully and acquired a satisfactory result. But, due to inadequacy of real data, we have done the experiments in an available database named DRIVE.

CHAPTER 8: GENERATION OF BIOMETRIC TEMPLATE

Retinal biometrics, being considered as one of the most reliable biometrics among all , using the unique biometric features of the retinal image , we have generated a 96 bytes template which will used as the main authentication key for proposed biometric security system.

Image captured from different angle may lead to even authentication failure. In the proposed system this problem can be resolved as the relative features of different biometric parameters of retinal images will be considered.

A 96 bytes template has been generated by extracting following different features from the retinal colored image.

- Relative distance between center of the optic disc and macula
- Distinct bifurcation points
- Bifurcation angle at every distinct bifurcation points

All this features have been concatenated to generate the secured 96 bytes template.

8.1 EXERIMENTAL RESULTS:

DATABASE (96 BYTES TEMPLATE FOR ALL THE IMAGES IN DRIVE DATABASE)(Table 11)

IMAGE NO	TEMPLATE
1	822472056429849882648499404871002471081012488410324059104204771042411510524490109389117115226751
2	484248217493026060191287522188823937985242921022836011934881223005126207112136232931403294314333
3	712982198529510799186569935056101229541082636511618667118137771181841031201855812313011112527697
5	672662177725455102173491062346010922925110238117113233571143517212531078128193101131191771471692
6	470255186552246379303769622744962645898293871012137610121870101220651032199211139159112413191152
7	483252131732364381198608120411384346909240357100359661033176611733894131102941344528214036847144
8	491282206105213961102079212238181125346621431667114846875155144591621071111692797617743477180431
9	782622077927982822965083300608522672942661129525555105364981292241081644418716941910817157801791
10	466281182962864099223711002175210515696131335891383657014335366145358631563977917238292190358731
11	63254221482087654189955420010857200556637850681712770173297439629753975978403218015627811557284 4
12	892631953525669702559089352889023262102269811213737713415277143147941463671081571434017011986176
13	49727521350252885723663652068571305677232645733081127630668903257396246661151288713239046135394 8
14	493315200643408081272838443411488440829521490107348621123398116418921427872148386851544429415445
16	491272199463065748317149315205031636601938365344146634537673444988211819837658983872410138253104
17	280470189722442578317828738386116299921173003120410131224103212933576133423861664425416744110516
18	478278190704036871384997338695743577374363427823773782397980383948320457121407901461556415690861
19	258486207622208372379238741032942049394206859540768102276841201498712235110513324777141247411491
21	256692116716741763189480333579327479962744998422811042237112319053124351801293451121403546415119
22	471284190543204910332982128384881374916313910093155379721563809616821569169206101170385621722309

24	481287200612986665306197033067731833678248838015675833047792209809221162933205499331104100220102
25	298466182633848978262728424540912497397382661003824610917795112238671214071011262698512641166128
26	74248213463237269244437224072973877110414063105329951252958215580931722698183978918427596187352 5
27	500283221382917655251851031629011819241201948134229881362161041439841162202701623375616718999183
28	486269198533019355265665925510261218118612215785195778733697923399094339711530386120252761213497
29	505289226803249694333131134477212028284129361771333575614738491624357019946282022779621345242192
30	469263185803606085365958626447983167010129851102305109104218461093106810944286112195461604166917
32	484262203109247731113679411637431117267531193821412028563123381512740165143125661574135619522310
33	466337986523993782225585316178831947933296398417801073109411536119122375391272417812837751137386
35	78266209522037486263608942945953138096256811031791081041928910426979105328251053308910612268107 2
37	5102822257335159901416990421639127992120190901211899212235889126170881273517012919071343133714 63
38	290499212532228955276777132799893245010240292132355861442694116334964175255481791335818243971984
39	282891936834710380367618236076872917990264699227799923405110112896102239821041787810617736114466
40	282486199483531372259958722698100414801024165912318290127243811324456914730484184412711852497818

CHAPTER 9.CONCLUSION:

9.1 SUMMARY

A novel framework is proposed for autonomous biometric authentication system in which biometric retinal template is generated by extracting different unique features from the retina like optic disc center, centre of macula, bifurcateion points, bifurcation angles etc. The performance of the proposed system is reasonably good and comparable with existing algorithms. We have proposed a novel method to detect the exact location of optic disc i.e., root pixel which will also be used as one of the unique biometric feature of the retinal image for the generation of template . An automatic and efficient detection of it plays a significant role for various reasons, like to locate other anatomical components in retinal images, for vessel tracking to diagnose many eye diseases even related to Diabetes and for registering the image for personal authentication Also, the position of Optic Disc can be used as a reference length for measuring distances in retinal images, especially from the location of macula. Keeping the importance of finding Optic Disc in mind, we have taken an initiative to locate an exact point, probably the center of it within the white bright region called Optic Disc. This work will count and keep track of the number of normal vessels around the around the optic disc. In this way, we may define a general statistics of the number count of blood vessels in a healthy human eye. The width of the vessels around the optic disc has been calculated which will help the ophthalmologists for earlier detection of the PDR. In future, we will concentrate on finding out other biometric feature for the template generation. Detection of only bifurcation points in a fundus image is a challenging task in true sense. The purpose of the work aims to avoid numerous unnecessary hazards of appraising crossover points as one of the crucial feature for authentication. Most of the literature shows the crossovers as their reliable authentication parameter. But in contrary, image capturing should always be from a fixed location and angle to avoid non-identification of the authentic source. Moreover, the patients suffers from diseases like hypertension, cardiovascular diseases and type II diabetes, often experience the change in crossover points of their retina which further increases the possibility of True Negative (TN) factor in authentication process. So to focus on only bifurcation point which is anatomically stable and never changes is an important issue. We have tried to accomplish this work successfully and acquired a satisfactory result. But, due to inadequacy of real data, we have done the experiments in an available database named DRIVE.

9.2 LIMITATION & FUTURE WORKS

We plan to improve the accuracy, complexity, efficiency, execution time of the algorithms. We will try to publish papers on segmentation of the blood vessels, localization of the optic disc and localization of the macula. We will integrate this software with hardware to develop a secured biometric authentication system. We plan to continue testing of the existing modules for this domain as well as future development of our proposed framework to obtain more promising results.